Screening for Cardiovascular Safety: A Structure−Activity Approach for Guiding Lead Selection of Melanin Concentrating Hormone Receptor 1 Antagonists

Philip R. Kym,*,† Andrew J. Souers,† Thomas J. Campbell,‡ John K. Lynch,† Andrew S. Judd,† Rajesh Iyengar,† Anil Vasudevan,† Ju Gao,† Jennifer C. Freeman,† Dariusz Wodka,† Mathew Mulhern,† Gang Zhao,† Seble H. Wagaw,§ James J. Napier,§ Sevan Brodjian,† Brian D. Dayton,† Regina M. Reilly,† Jason A. Segreti,‡ Ryan M. Fryer,‡ Lee C. Preusser,‡ Glenn A. Reinhart,‡ Lisa Hernandez,⊥ Kennan C. Marsh,⊥ Hing L. Sham,† Christine A. Collins,† and James S. Polakowski‡

Global Pharmaceutical Research and Development, Abbott Laboratories, 100 Abbott Park Road, Abbott Park, Illinois 60064

Received December 8, 2005

An inactin-anesthetized rat cardiovascular (CV) assay was employed in a screening mode to triage multiple classes of melanin-concentrating hormone receptor 1 (MCHr1) antagonists. Lead identification was based on a compound profile producing high drug concentration in both plasma (>40 μM) and brain (>20 μg/g) with <15% change in cardiovascular endpoints. As a result of these stringent requirements, lead optimization activities on multiple classes of MCHr1 antagonists were terminated. After providing evidence that the cardiovascular liabilities were not a function of MCHr1 antagonism, continued screening identified the chromone-substituted aminopiperidine amides as a class of MCHr1 antagonists that demonstrated a safe cardiovascular profile at high drug concentrations in both plasma and brain. The high incidence of adverse cardiovascular effects associated with an array of MCHr1 antagonists of significant chemical diversity, combined with the stringent safety requirements for antiobesity drugs, highlight the importance of incorporating cardiovascular safety assessment early in the lead selection process.

Introduction

Melanin-concentrating hormone (MCH) is a cyclic, 19-amino acid peptide that is synthesized in cell bodies in the lateral hypothalamus and zona incerta of the central nervous system (CNS). MCH-peptide is now understood to play a major role in body weight regulation in rodents.[1,2] A single injection of MCH into the CNS stimulates food intake in rodents,[3] and chronic administration leads to increased body weight.[4] Similarly, transgenic mice altered to increase expression of the MCH gene are susceptible to insulin resistance and obesity.[5] In contrast, mice lacking the gene encoding MCH are hypophagic, are lean, and maintain elevated metabolic rates.[6] Consistent with this phenotype, genetically altered animals that lack the gene encoding the MCH receptor (MCHr1) maintain elevated metabolic rates and thus remain lean, even though they are hyperphagic on a normal diet.[7,8] Finally, the observation that chronic administration of small-molecule antagonists leads to the reduction of body weight provides further validation of MCHr1 blockade as a novel target for antiobesity pharmacotherapy.[9]

Previously, we have identified several structurally diverse classes of compounds with affinity for MCHr1.[10−13] Several of these unique chemotypes were subsequently optimized to afford compounds with high affinity for MCHr1, potent functional inhibition of MCH-mediated Ca^{2+} release, and good oral bioavailability in both mouse and rat pharmacokinetic studies. Furthermore, several analogues from distinct classes of MCHr1 antagonists conferred dose-dependent weight loss in diet-induced obese (DIO) mice upon oral administration in 14 day efficacy studies (Chart 1).

Chart 1

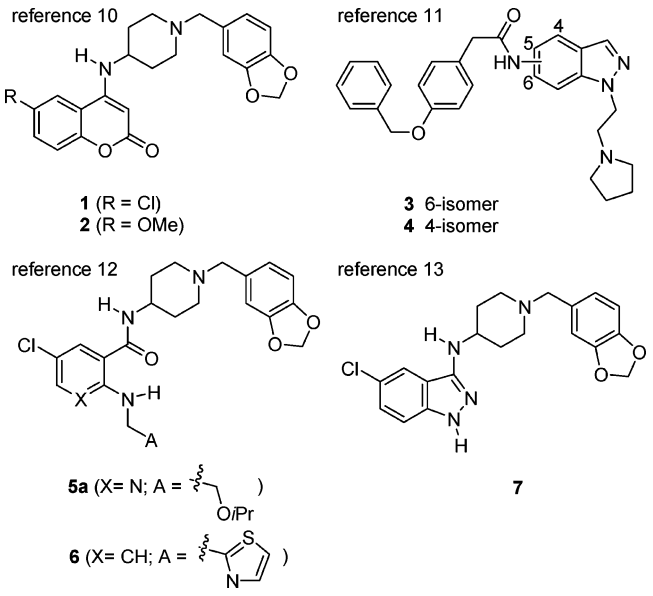

Following the identification of orally efficacious MCHr1 antagonists from structurally distinct series, we proceeded to evaluate several lead compounds in a pentobarbital-anesthetized dog model of cardiovascular function using an escalating dosing paradigm.[14] Compounds were evaluated for cardiovascular liabilities dosing up to plasma concentrations 30-fold above the estimated efficacious plasma C_{max} in DIO mice. Previously, we have described the dog cardiovascular profiles of aminopiperidine coumarin analogues **1** and **2**.[10] Unfortunately, despite appearing to be well tolerated upon oral dosing in chronic efficacy studies, these compounds caused hemodynamic effects at low multiples of their corresponding therapeutic plasma concentrations, thus obviating any further development. Interestingly, a structurally related, yet MCHr1 inactive, analogue demonstrated a similar profile in the pentobarbital-anesthetized

* To whom correspondence should be addressed. Philip R. Kym, Abbott Laboratories, Department R4MF; Bldg. AP10, 100 Abbott Park Road, Abbott Park, IL 60064-6099. Tel: (847)-935-4699. Fax: (847)-938-1674. E-mail: phil.kym@abbott.com.

† Metabolic Disease Research.

‡ Integrative Pharmacology.

§ Process Chemistry.

⊥ Exploratory Pharmacokinetics.

10.1021/jm0512286 CCC: $33.50 © 2006 American Chemical Society
Published on Web 03/11/2006

Scheme 1[a]

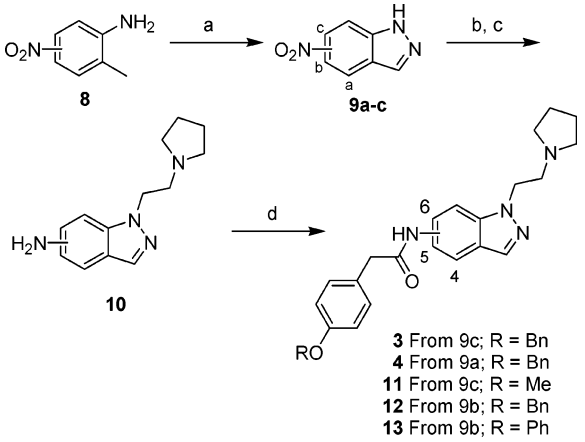

[a] Reagents and conditions: (a) $NaNO_2$, AcOH, rt, 95%; (b) chloroethylpyrrolidine hydrochloride, K_2CO_3, DMF, 60 °C, then chromatography, 27−67%; (c) Fe, NH_4Cl, 65 °C; (d) RCO_2H, EDCI, HOBt, DMF, NMM, 56−89%.

dog cardiovascular model, suggesting that the observed cardiotoxicity was linked to the particular structural chemotype and not to MCHr1 activity.[10] The adverse cardiovascular safety profiles observed in the pentobarbital-anesthetized dog cardiovascular model at low drug concentrations revealed a significant challenge for this program. Furthermore, since considerable time and resources had been applied to compound optimization prior to assessment of cardiovascular safety, we identified the need to screen compounds for cardiovascular liabilities at a much earlier stage in our lead optimization program. To this end, we have incorporated a medium throughput, cardiovascular screening assay in inactin-anesthetized rats to eliminate compounds with cardiovascular liabilities early in the lead prioritization process. Over 130 compounds from multiple unique chemical series were evaluated in the inactin-anesthetized rat cardiovascular screening assay, and structure−activity relationships of the parameters responsible for cardiovascular liabilities were established. This method of early screening reflects a high priority on cardiovascular safety and represents a new strategy for rapidly triaging lead series in a discovery program.

Chemistry

The general synthetic approach to the indazole amides is outlined in Scheme 1.[11] Briefly, 4-nitroindazole (**9a**) was synthesized from 3-nitro-*o*-tolylamine and sodium nitrite, while the 5- and 6-nitroindazoles (**9b** and **9c**, respectively) were obtained from commercial sources. Alkylaton of the nitroindazole cores (**9**) with 2-chloroethylpyrrolidine hydrochloride afforded a mixture of N^1 and N^2-alkylated isomers in ratios that varied by the position of the nitro substituent. After chromatographic separation and isolation of each isomer, iron-mediated reduction afforded the individual anilines **10**, and amide bond formation furnished the final products **3**, **4**, and **11**−**13**.

The indazole urea analogues were synthesized in an analogous manner by first alkylating 5-nitroindazole (**9b**) with the appropriate aminoethyl chloride followed by chromatographic separation of the N^1 and N^2 isomers (Scheme 2). Iron-mediated reduction afforded the corresponding anilines **14a**,**b**, and reaction with phenoxyphenylisocyanate furnished the urea products **15**−**17**.

For compounds **19** and **20**, a reductive amination strategy was utilized. As shown in Scheme 3, 5-nitroindazole (**9b**) was alkylated with 1,1′-dimethoxy-2-bromoethane, and the desired N^1- or N^2-functionalized isomers were isolated via chromatography. Following iron-mediated reduction and urea formation via isocyanate coupling with the desired aniline (**18**), the latent aldehyde was liberated with aqueous acid. Reductive amination with secondary amines afforded the final compounds.

Scheme 2[a]

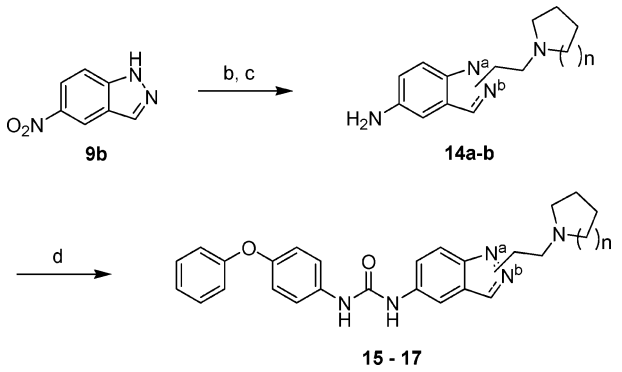

[a] Reagents and conditions: (a) Chloroethylpyrrolidine hydrochloride or chloroethylpiperidine hydrochloride, K_2CO_3, DMF, 60 °C, then chromatography, 27−67%; (c) Fe, NH_4Cl, 65 °C; (d) $PhOC_6H_4NCO$, THF, 60 °C, 90%.

Scheme 3[a]

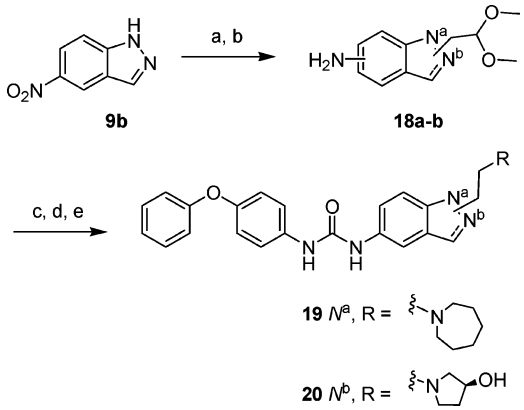

[a] Reagents and conditions: (a) 1,1′-Dimethoxy-2-bromoethane, K_2CO_3, DMF, 60 °C, then chromatography (41−57%); (b) Fe, NH_4Cl, 65 °C, 90%; (c) $PhOC_6H_4NCO$, THF, 85%. (d) 2:1 2N HCl:acetone, 60 °C; (e) R_1R_2NH, MeOH (1% AcOH), MP-$CNBH_3$.

Representatives of the 4-aminopiperidine classes of MCHr1 antagonists were synthesized from a common precursor as outlined in Scheme 4. Briefly, 4-*N*-Boc-aminopiperidine was reacted with piperonal under reductive amination conditions to afford the corresponding benzylamine. Deprotection with HCl afforded the primary amine **22**, which could then be coupled with heterocyclic halides or acids using amide coupling or palladium-mediated coupling conditions to afford the final compounds **5a** (for synthesis of **5b**, see Supporting Information section III), **6**, **24**−**25**, and **23**, respectively. To obtain compound **6**, 5-isotoic anhydride was reacted with amine **22**, followed by reductive amination to afford the final product. Finally, the synthesis of compounds **2**[10] and **7**[13] have been reported elsewhere.

Results and Discussion

Magnitude of the Cardiovascular Problem. Prior to making significant changes in our lead optimization strategy, we investigated the option of circumventing the cardiovascular issues simply by changing the chemotype of our lead series. The project team selected an efficacious lead compound (**4**) from a structurally unique aminoalkylindazole series for cardiovascular safety evaluation in the pentobarbital-anesthetized dog

Scheme 4[a]

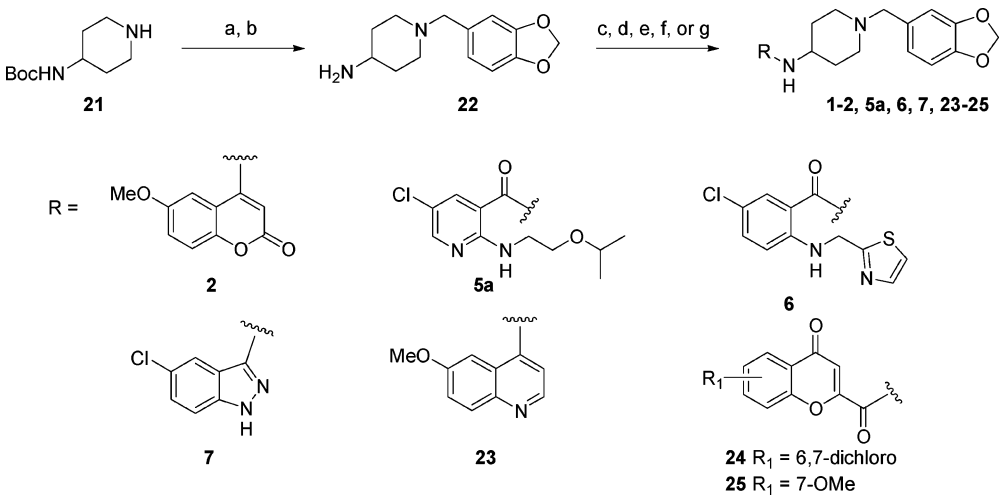

[a] Reagents and conditions: For **5a**: (a) Piperonal, Na_2SO_4, AcOH, $NaB(OAc)_3H$; (b) TFA, CH_2Cl_2, then HCl (>100%); (c) i. RCOOH, PS-DCC, HOBt, DMF, 25 °C, 95%; ii. RNH_2, CH_3CN, 150 °C, 30 min, microwave, 31%; For **6**: (d) 5-Chloroisatoic anhydride, CH_3CN, 80 °C, (e) RCHO, $NaBH_3CN$, MeOH, 50 °C, 21%; For **23**: (f) RBr,[15] Pd $(OAc)_2$, BINAP, NaO*t*Bu, PhMe, 80 °C, 64%; For **24**, **25**: (g) RCOOH, EDCI, HOBt, NMM, DMF, 25 °C, 72−81%.

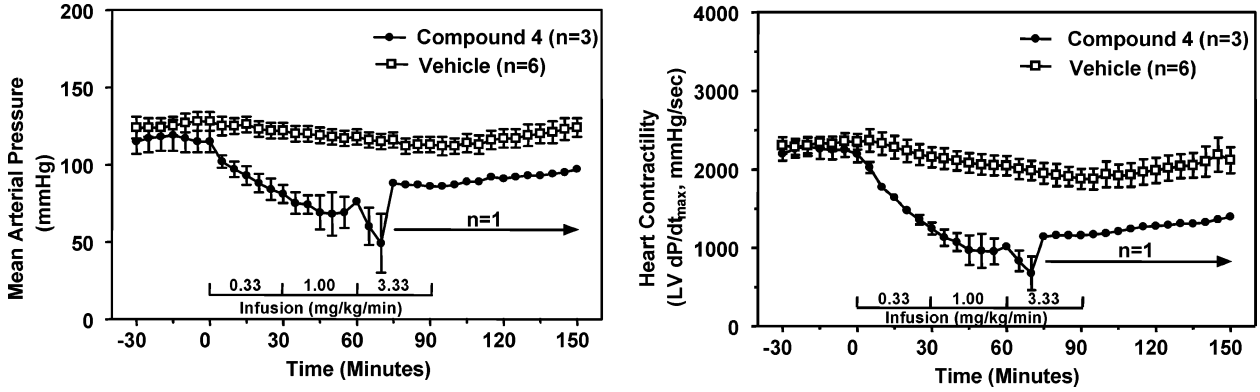

Figure 1. The functional effects of intravenous administration of **4** were assessed in male beagle dogs anesthetized with sodium pentobarbital (35 mg/kg; 6 mg/kg/h maintenance infusion). Animals were intubated, mechanically ventilated, and instrumented for acute measurement of mean arterial pressure and cardiac contractile function. Following a 30-min baseline period, **4** was infused as a series of three 30-min infusions followed by a 60-min posttreatment period.

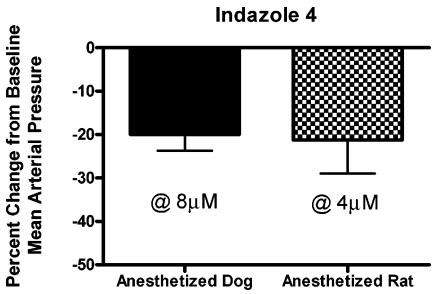

Figure 2. Comparison of peak decreases in mean arterial pressure (MAP) observed in the pentobarbital-anesthetized dog and inactin-anesthetized rat for indazole **4** ($n = 3$ for both species). Data expressed as mean ± SEM. Numbers at the bottom of the bar graphs are the mean plasma concentrations associated with the decreases in MAP.

model. Once again, despite the absence of observable negative effects in a 14 day efficacy study, this compound caused profound reductions in mean arterial pressure and heart contractility during the first 30 min infusion. (Figure 1).

The adverse cardiovascular profiles observed with clearly distinct chemotypes of MCHr1 antagonists raised several questions for the project team: (1) what is the source of the cardiovascular problems?; (2) could we identify an effective method to screen for adverse cardiovascular events early in our lead optimization process?; and (3) are the observed cardiovascular liabilities inherently linked to MCHr1 antagonism?

Cardiovascular Screening: Strategic Considerations. Considerable effort was made to assign the observed cardiovascular toxicity to cross-reactivity at specific receptors, transporters, and/or ion channels via CEREP-panel[16] and hERG[17] affinity screening. Unfortunately, this effort was unsuccessful, as cross-reactivity of analogues across different chemotypes and within subseries proved highly variable. We were unable to identify a receptor, transporter, or ion channel for which activity of the studied compounds would correlate with observed hemodynamic effects. Consistent with this observation, toxicity could also not be attributed to the general state of mast-cell degranulation driven by the release of histamine (data not shown). Finally, the profiles of aminopiperidine coumarins **1** and **2**[10] and aminoalkylindazole **4** (Figure 1) in the pentobarbital-anesthetized dog assay, which produced effects on both the peripheral vasculature (decrease in MAP) and direct cardiac effects (changes in d*P*/d*t*), suggested that the cardiovascular effects were not solely attributed to a postsynaptic vasodilatory effect on vascular smooth muscle. Therefore, an in vitro measurement, such as an isolated dog femoral artery assay or assay of cross-reactivity at a single ion channel or receptor would not adequately predict the in vivo cardiovascular effects of these

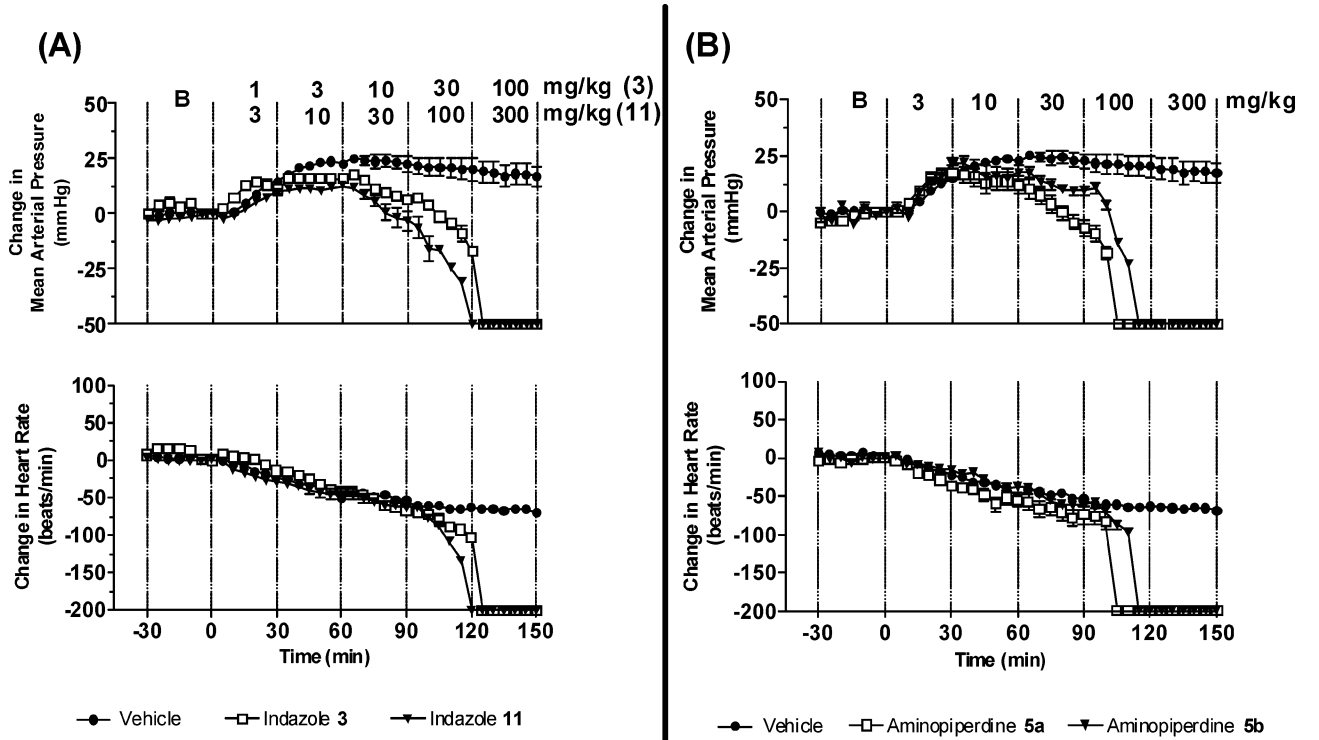

Compd.	Ca^{2+} Release	EOS [Plasma] μM	EOS [Brain] μg/g
3	IC_{50} 11 ± 2nM	23 ± 4	10 ± 2
11	14% inh. @10μM	39 ± 9	6 ± 2

Compd.	Ca^{2+} Release	EOS[a] [Plasma] μM	EOS [Brain] μg/g
5a	IC_{50} 25 ± 6nM	44 ± 20	88 ± 12
5b	30% inh. @10μM	61 ± 3	138 ± 13

Figure 3. Comparison of MCHr1 active and inactive analogues within the indazole (A) and aminopiperidine (B) chemical series on mean arterial pressure (MAP) and heart rate (HR) in inactin-anesthetized rats. Tables at the bottom of each figure show in vitro potency (Ca^{2+} release) and end of study (EOS) plasma and brain levels for each compound. Data expressed as mean ± SEM.

Chart 2

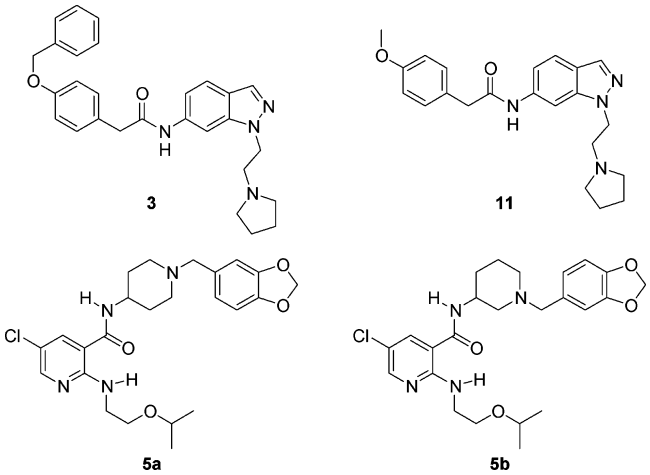

compounds. Thus, our strategic decision was to prioritize development of a whole-animal screening model that would identify compounds that had inherently safer cardiovascular profiles.

Hence, we sought to implement a higher throughput and less compound-intensive, whole-animal model that could be applied as an early screening tool. The acutely instrumented anesthetized rat cardiovascular model[18,19] is a predictive in vivo model of cardiovascular function that effectively interrogates lead molecules for undesirable cardiovascular effects. Studies are conducted under anesthesia (inactin) using a series of intravenous infusions and periodic collection of small (150 μL) blood samples to assess active drug levels, providing concentration−response functions for clinically relevant endpoints of blood pressure and heart rate. The model's predictive value arises from its ability to identify compounds that exert marked adverse effects on cardiovascular function at relevant doses or plasma concentrations, results that would preclude further lead optimization. One significant advantage of the anesthetized rat model is that it requires significantly less compound (<200 mg) per assay than the anesthetized dog assay (multigram quantities). In addition, easier access to animals and reduced instrumentation contribute to a greater capacity for compound throughput in the anesthetized rat assay compared to the dog assay. Therefore, from a technical standpoint, we hypothesized that the inactin-anesthetized rat model could be used as an effective screening model to establish structure−activity relationships (SAR) regarding cardiovascular effects.

Before undertaking a screening effort using the inactin-anesthetized rat, it was important to determine if the cardiovascular effects observed for MCHr1 antagonists would be similar to those observed in the pentobarbital-anesthetized dog.[14] Aminoalkylindazole **4** was selected as an initial compound for evaluation in both the anesthetized dog and rat models. This compound represents a potent MCHr1 antagonist with a functional IC_{50} (Ca^{2+} release) of 239 ± 40 nM. Intravenous infusion of indazole **4** in pentobarbital-anesthetized dogs produced large decreases in mean arterial pressure (MAP) and

Chart 3

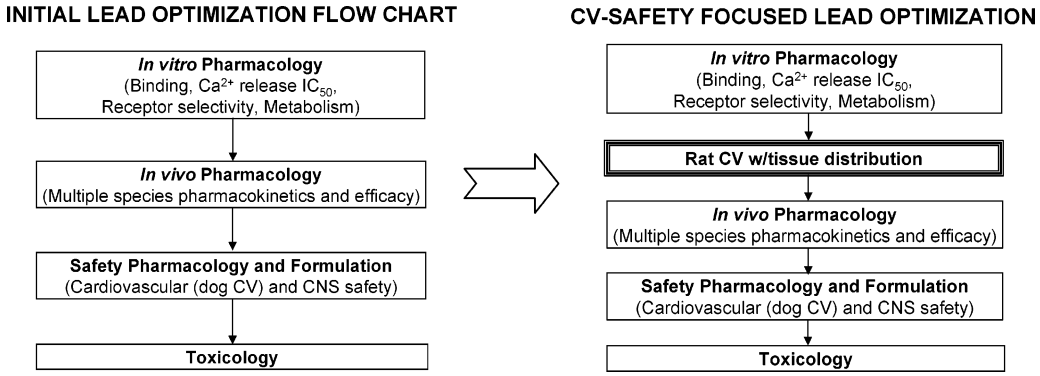

Table 1

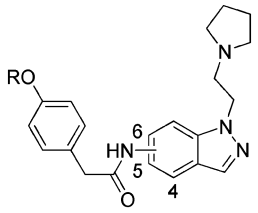

3, 4, 11-13

Compd	Pos	R	Binding IC_{50} (nM)[b,d]	Ca^{2+} release IC_{50} (nM)[c,d]	No-Effect Dose (mg/kg)[e]	EOS severity[f] (MAP)	EOS Plasma (μM)	EOS Brain (μg/g)
3	6	$C_6H_5CH_2$-	1.4 ± 0.4	11 ± 2	10	↓↓↓	23 ± 4	10 ± 2
4	4	$C_6H_5CH_2$-	25 ± 10	71 ± 35	60	↓↓↓	4 ± 0. 4	NA[g]
11	6	CH_3-	3628 ± 799	> 10,000	30	↓↓↓	39 ± 9	6 ± 2
12	5	$C_6H_5CH_2$-	558 ± 79	14% inh @ 10 μM	30	↓↓↓	53 ± 4	46 ± 8
13	5	C_6H_5-	78 (74, 82)[h]	309 (254, 364)[h]	60	↓↓	2 ± 0.2	NA[g]

[a] All compounds were >95% pure by HPLC and characterized by ^{1}H NMR and passed combustion analysis requirements. [b] Displacement of [^{125}I]-MCH from MCHr1 expressed in IMR-32 (I3.4.2) cells (MCH binding K_d = 0.66 ± 0.25 nM, B_{max} = 0.40 ± 0.08 pmol/mg). [c] Inhibition of MCH-mediated Ca^{2+} release in whole IMR-32 cells (MCH EC_{50} = 62.0 ± 3.6 nM). [d] All values are mean values ± SEM and are derived from at least three independent experiments (all duplicates). [e] Animals were treated with escalating doses of compounds from 0 to 100 mg/kg. The highest doses achieved without cardiovascular effects are reported. [f] EOS (end of study) refers to the point at which the infusion was terminated. EOS severity: severity of separation from vehicle at the termination of the study; ↓ = <15% change from vehicle; ↓↓ = 15−25% change from vehicle; ↓↓↓ = >25% change from vehicle. [g] NA, not assayed. [h] Mean value of two determinations that are provided in parentheses.

cardiac contractility (d*P*/d*t*) at relatively low plasma concentrations. Depressor and negative inotropic effects began at plasma concentrations less than 8.1 ± 0.9 μM and deviation from baseline continued in a concentration-dependent manner (Figure 1). The infusion of indazole **4** required termination once plasma concentrations reached 36.3 ± 3.9 μM since the depressor and contractility effects decreased over 50% compared to baseline values.[19] In the inactin-anesthetized rat cardiovascular screening paradigm (three rats tested per compound), indazole **4** produced sharp decreases in MAP and d*P*/d*t* at 4.0 ± 0.4 μM μg/mL plasma concentrations (Figure 2). Hence, escalating doses of indazole **4** in both anesthetized dogs and rats produced qualitatively similar decreases in MAP and cardiac contractility at low plasma concentrations.

Prior to launching an extensive screening campaign to identify MCHr1 active analogues with an improved cardiovascular profile, we sought to address the question of whether the observed cardiovascular toxicity was inherently linked to MCHr1 blockade. To maximize throughput, the model was streamlined to focus on MAP and heart rate, clinically relevant endpoints requiring minimum instrumentation to monitor. Because MCHr1 is highly concentrated in the lateral hypothalamus, we chose to monitor the end-of-study (EOS) drug concentration in whole brain in addition to periodic collection of blood samples to assess plasma drug levels associated with escalating dosing. We evaluated the cardiovascular profiles of structurally similar sets of MCHr1 active and inactive analogues in two different lead series in the inactin-anesthetized rat model.

Table 2

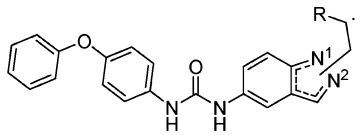

Compd	R	N	Binding IC_{50} (nM)[b,d]	Ca^{2+} release IC_{50} (nM)[c,d]	No-Effect Dose (mg/kg)[e]	EOS severity[f] (MAP)	EOS Plasma (μM)	EOS Brain (μg/g)
15		1	12 ± 3	104 ± 25	100[i]	↓↓↓	88 ± 18	10 ± 1
16		1	5 (3, 7)[h]	136 ± 39	30	↓↓↓	77 ± 5	13 ± 1
19		1	4 ± 2	103 ± 40	3	↓↓	NA[g]	NA[g]
17		2	46 (43, 48)[h]	314 ± 77	100[i]	↓↓	558 ± 178	6 ± 1
20		2	57 (56, 59)[h]	214 (134, 294)[h]	No effect	No effect	201 ± 53	3 ± 1

[a] All compounds were >95% pure by HPLC and characterized by ^{1}H NMR and passed combustion analysis requirements. [b] Displacement of [^{125}I]-MCH from MCHr1 expressed in IMR-32 (I3.4.2) cells (MCH binding K_d = 0.66 ± 0.25 nM, B_{max} = 0.40 ± 0.08 pmol/mg). [c] Inhibition of MCH-mediated Ca^{2+} release in whole IMR-32 cells (MCH EC_{50} = 62.0 ± 3.6 nM). [d] All values are mean values ± SEM and are derived from at least three independent experiments (all duplicates). [e] Animals were treated with escalating doses of compounds from 0 to 100 mg/kg. The highest doses achieved without cardiovascular effects are reported. [f] EOS (end of study) refers to the point at which the infusion was terminated. EOS severity: severity of separation from vehicle at the termination of the study; ↓ = < 15% change from vehicle; ↓↓ = 15−25% change from vehicle; ↓↓↓ = > 25% change from vehicle. [g] NA, Not Assayed. [h] Mean value of two determinations that are provided in parentheses. [i] Animals were treated with escalating doses of compounds from 0 to 300 mg/kg.

In the aminoalkylindazole series, the exceptionally potent MCHr1 antagonist **3**[11] produced sharp decreases in MAP early in the dose range (10 mg/kg, Figure 3). Just prior to reaching the 30 mg/kg dose, MAP fell below the minimum pressure limit,[20] and the infusions were terminated; average drug concentrations at the end of the study were 23 ± 4 μM (plasma) and 10 ± 2 μg/g (brain). The structurally related, but MCHr1 inactive, analogue **11** (14% inhibition of MCHr1-mediated Ca^{2+} release @ 10 μM) also produced a sharp decrease in MAP leading to termination of the infusion at comparable plasma (39 ± 9 μM) and brain (6 ± 2 μg/g) concentrations (Figure 3).

In a second lead series represented by the aminopiperidine benzamides **5a** (Ca^{2+} release IC_{50} = 16 nM) and **5b** (30% inhibition @ 10 μM), similar deleterious effects on cardiovascular function also occurred at comparable drug concentrations. Escalating doses of the MCHr1 active analogue **5a** resulted in a steep decline in MAP beginning at the 30 mg/kg dose. The concentrations that led to this effect were 44 ± 19 μM (plasma) and 88 ± 12 μg/g (brain), while escalating doses of the MCHr1 inactive analogue **5b** resulted in cardiovascular effects at comparable drug concentrations of 61 ± 3 μM (plasma) and 138.1 μg/g (brain). Each of the inactive analogues (**11** and **5b**) conferred similar cardiovascular liabilities relative to the corresponding lead structures (**3** and **5a**, respectively), providing further evidence that the observed hemodynamic effects were structure related, and not linked to MCHr1 activity.

Since the inactin-anesthetized rat provided a qualitatively predictive cardiovascular profile to that observed in the pentobarbital-anesthetized dog, and our initial data suggested that the cardiovascular effects were not linked to MCHr1 activity, an intense screening effort was initiated using the rat to provide rapid structure−activity relationships (SAR) with respect to cardiovascular events. The objective was to eliminate compounds that demonstrated cardiovascular liabilities in the anesthetized-rat screening assay prior to evaluating compounds in pharmacokinetic and in vivo efficacy assays (Chart 3). As an additional filter, since the targeted site of action is the lateral hypothalamus, we required that analogues demonstrate a safe cardiovascular profile while attaining high drug concentration in the brain. Over 130 compounds from multiple unique chemical series were evaluated in the anesthetized-rat cardiovascular screening assay, and structure−activity relationships of the parameters responsible for cardiovascular liabilities were established. Thus, in the remaining sections of this paper, we describe the rat cardiovascular SAR, focusing on MAP and heart rate (HR) with plasma and brain drug level analysis, for two distinct series of MCHr1 active antagonists, aminoalkylindazoles and piperonyl-substituted 4-aminopiperidines.

Aminoalkylindazoles. Several members of aminoalkylindazole series demonstrated excellent in vivo efficacy in a two-week model for weight loss in DIO mice.[11,21] Despite the absence of any apparent toxicity following semichronic oral dosing (14 days),[11] these compounds produced severe cardiovascular effects at low multiples of their corresponding efficacious plasma concentrations. Specifically, the occurrence of hemodynamic effects at low plasma concentrations for **3** and **4** (Table 1), in addition to the effects observed upon infusion of the inactive analogue **11** indicated that the cardiovascular toxicity was possibly a result of the structural features of the indazole amide compounds. Further evidence for this was

provided by the infusion of indazole **12**, the 5-positional regioisomer characterized by lesser binding affinity and negligible functional potency. Despite the difference in activity, indazole **12** demonstrated a similar cardiovascular profile compared to isomers **3** and **4**, with large depressor effects on MAP and HR becoming apparent during the 30 to 100 mg/kg infusion period.

The consistent profile of MAP and HR depressor effects at low plasma concentrations for amides **3**, **4**, and **11** prompted us to further explore the effects of minor perturbations to the side chain and the alkylaminoethyl substituent. As described in a previous report,[11] contraction of the amide side chain from a benzyloxy to a phenoxy group in 5-substituted analogues (such as **12** to **13**) rescued the in vitro activity to a significant extent (Table 1). Infusion of this truncated analogue had no deleterious effects on the MAP or HR of the rats until the 60 mg/kg infusion. At this time, both parameters rapidly decreased until all animals dropped below the minimum pressure limit. Interestingly, the EOS plasma concentration was only 2.0 ± 0.2 μM. The drastic effects at low plasma concentration reiterated the deleterious effects of amide side chains within the series. This prompted the cardiovascular assessment of compounds containing amide replacements, such as urea analogue **15**,[21] a compound characterized by good binding affinity and functional potency. As highlighted in Table 2, MAP was unaffected until the beginning of the 100 mg/kg infusion, after which it began to decline steadily. Heart rate was unaffected throughout the study. Although one animal did fall below the minimum MAP limit and predicated termination of the infusion, the overall profile was substantially improved relative to that of the amide analogues. Additionally, the compound attained an end of study plasma concentration of 88 ± 18 μM, indicating that this compound was safer with respect to the measured parameters when compared to the representatives of the amide series.

Encouraged by the observation that the urea side chain conferred heightened tolerability upon intravenous (iv) infusion, we then explored modifications to the aminoalkyl region of the compound. Representative examples include the six- and seven-membered heterocycles **16** and **19**, respectively, which are both of comparable in vitro potency to **15**. Interestingly, both compounds were substantially worse from a tolerability standpoint than pyrrolidine **15**. While piperidine **16** had no effect on MAP and HR at lower doses, a steady and dose dependent decrease in MAP started at the 30 mg/kg infusion and continued throughout the study, culminating in the termination of one animal's infusion. A dose dependent decrease in HR occurred within a similar time frame, although the effects were not as drastic as for the MAP parameter. Interestingly, the EOS plasma and brain concentrations were very similar to those of **15**, demonstrating the pronounced differences in in vivo effects between compounds with very minor structural differences. Infusion of the seven-membered analogue **19** conferred depressor effects on MAP at an earlier time frame, with significant decreases appearing within the first infusion.

Because of the improved cardiovascular safety profile of the indazole urea **15**, we next explored the safety profile of the N^2-alkylated regioisomer **17**. Similar to **15**, no effects on MAP or HR were observed throughout the first four periods of infusion, although a steep decline in MAP became evident during the 30 to 100 mg/kg infusion. However, as shown in Table 2, EOS plasma levels were considerably higher than those observed with previous analogues (558 ± 178 μM). This result suggested that very high plasma drug concentration of **17** was required to confer deleterious effects on MAP or HR. Although the brain-to-plasma ratio was suboptimal, the increased safety with this N^2-alkylated urea prompted further exploration of analogues of **17**. Since the one and two carbon homologues of the N^1-alkylated urea conferred more adverse cardiovascular effects relative to the parent pyrrolidine **15**, we turned our attention to substituted pyrrolidine analogues. Screening of multiple ureido-substituted indazoles led to the identification of **20**, which was similar in binding and functional potency to **17**. Infusion of this compound conferred no significant effects on MAP and HR throughout the experiment (Figure 4), and pharmacokinetic analysis revealed high drug levels in the plasma (201 ± 53 μM), albeit with lower levels in the brain (3 ± 1 μg/g).

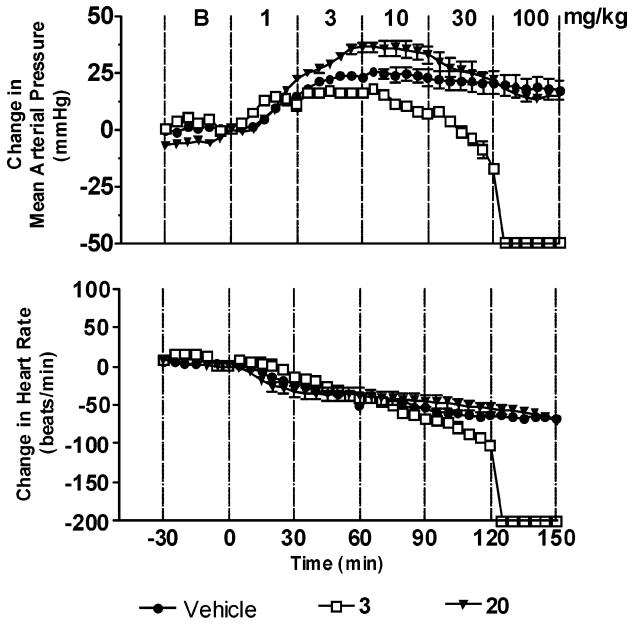

Compd.	Ca^{2+} Release	EOS [Plasma] μM	EOS [Brain] μg/g
3	IC_{50} 11 ± 2nM	23 ± 4	10 ± 2
20	IC_{50} 214 ± 80nM	201 ± 53	3 ± 1

Figure 4. Comparison of indazole analogue **3** and optimized analogue **20** on MAP and HR in inactin-anesthetized rats with relative potencies and achieved EOS plasma and brain levels for each compound. Data expressed as mean ± SEM.

Analogue **20** demonstrated significantly enhanced cardiovascular safety relative to the starting analogue **3** and passed the critical barrier of conferring no side effects within the limits of infusion while maintaining high EOS levels of drug in the plasma. Consequently, this analogue was put forward for pharmacokinetic analysis in DIO mice in order to assess oral plasma and brain exposure in preparation for in vivo efficacy studies. Dosing at 10 mg/kg in the animals and subsequent analysis, however, revealed negligible brain penetration in DIO mice (plasma AUC 1.02 μg·h/mL; brain AUC 0 μg·h/g), thus obviating the need to test this compound for weight loss in an efficacy study. Evaluation of multiple analogues of **20** afforded similar results, and further SAR efforts to retain the safety profile while improving the brain penetration were fruitless. Therefore, the series was deemphasized, and we turned toward alternative classes of MCHr1 antagonists.

Aminopiperidines. While the effort to identify analogues with minimal effects on the rat cardiovascular system at high drug concentrations in the plasma and brain was compromised in the aminoalkylindazole lead series due to the low brain

Table 3

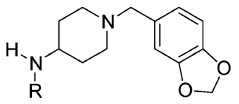

Compd	R	Binding IC_{50} (nM)[b,d]	Ca^{2+} release IC_{50} (nM)[c,d]	No-Effect Dose (mg/kg)[e]	EOS severity[f] (MAP)	EOS Plasma (μM)	EOS Brain (μg/g)
2	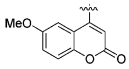	2 ± 1	11 ± 1	30	↓↓↓	272 ± 12	71 ± 11
5a	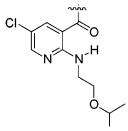	6 ± 2	25 ± 6	10	↓↓↓	44 ± 19	88 ± 12
6	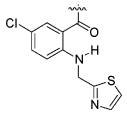	2 ± 1	53 ± 11	3	↓↓	91± 6	NA
7		16 ± 7	376 ± 81	3	↓↓↓	22 ± 2	30 ± 5
23	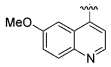	10 ± 1	74 ± 6	3	↓↓↓	NA[g]	NA[g]
24	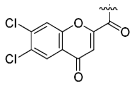	3 ± 2	83 ± 8	No effect	No effect	42 ± 4	63 ± 14
25	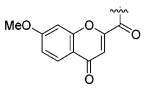	6 ± 2	73 ± 16	No effect	No effect	66 ± 5	158 ± 13

[a] All compounds were >95% pure by HPLC and characterized by ^{1}H NMR and passed combustion analysis requirements. [b] Displacement of [^{125}I]-MCH from MCHr1 expressed in IMR-32 (I3.4.2) cells (MCH binding $K_d = 0.66 \pm 0.25$ nM, $B_{max} = 0.40 \pm 0.08$ pmol/mg). [c] Inhibition of MCH-mediated Ca^{2+} release in whole IMR-32 cells (MCH $EC_{50} = 62.0 \pm 3.6$ nM). [d] All values are mean values ± SEM and are derived from at least three independent experiments (all duplicates). [e] Animals were treated with escalating doses of compounds from 0 to 100 mg/kg. The highest doses achieved without cardiovascular effects are reported. [f] EOS (end of study) refers to the point at which the infusion was terminated. EOS severity: severity of separation from vehicle at the termination of the study; ↓ = <15% change from vehicle; ↓↓ = 15−25% change from vehicle; ↓↓↓ = >25% change from vehicle. [g] NA, not assayed.

exposure of the safest analogues, our experience with this lead series provided a clear demonstration of the utility of the rat cardiovascular assay in a screening mode to identify analogues with improved cardiovascular profiles. Hence, we embarked on an effort to evaluate the rat cardiovascular profiles of MCHr1 antagonists from multiple chemotypes that had been identified from both our internal efforts and the external literature. One of the preferred pharmacophores that has repeatedly appeared in MCHr1 active compounds is a piperonyl-substituted 4-aminopiperidine fragment.[10,22] We chose to use this fragment to screen for heterocyclic groups that would lead to potent MCHr1 antagonists demonstrating both novel structure and pharmacological properties. This strategy led to the rapid identification of multiple analogues that demonstrated high affinity for MCHr1 and potent functional antagonism (Table 3).

Evaluation of these new classes of heterocycle-substituted 4-aminopiperidine MCHr1 antagonists in the rat cardiovascular screening assay revealed an interesting SAR. Attempts to replace the coumarin ring system with either a 3-subsituted indazole (**7**) or a 4-subsituted quinoline (**23**) afforded analogues that were MCHr1 active but demonstrated deleterious cardiovascular effects at low doses. Beginning with the 3 mg/kg dose, these analogues caused severe cardiovascular depressor effects on both MAP and HR (Table 3). These effects occurred at significantly lower dose ranges and final plasma concentrations than we had previously observed with the aminopiperidine coumarin **2**.

Next, we investigated the effect of replacing the bicyclic heterocycle with either the monocyclic *o*-amino nicotinamide (**5a**) or *o*-amino benzamide (**6**), taking advantage of the intramolecular hydrogen bond to mimic the second ring. Once again, these analogues demonstrated potent MCHr1 antagonism, yet still caused severe depressor effects on MAP at doses as low as 3 mg/kg. We were pleased, however, to identify a series of chromone substituted amides (**24** and **25**) that were characterized by a fundamentally different profile in the rat cardiovascular assay. The chromone-substituted aminopiperidine amides demonstrate high affinity for MCHr1 and potent functional antagonism, but confer only limited effects on the rat cardiovascular

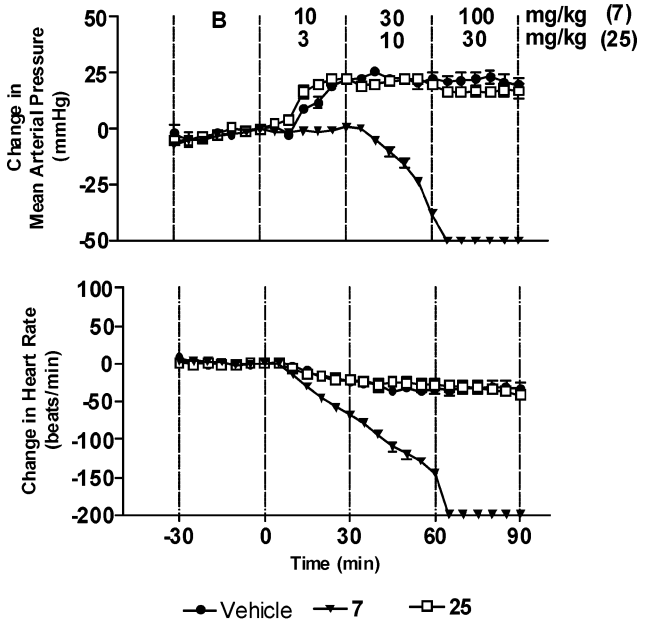

Compd.	Ca^{2+} Release		EOS [Plasma] μM	EOS [Brain] μg/g
7	IC_{50}	376 ± 81nM	22 ± 2	30 ± 15
25	IC_{50}	73 ± 16nM	66 ± 5	158 ± 13

Figure 5. Comparison of indazole-substituted aminopiperidine **7** with the chromone-substituted aminopiperidine amide **25** on MAP and HR in inactin-anesthetized rats with relative potencies and achieved EOS plasma and brain levels for each compound. Data expressed as mean ± SEM.

system even at very high drug concentrations in both the plasma and the brain. The 6,7-dichlorochromone analogue **24** achieved an EOS brain concentration of 63 ± 14 μg/g without changing MAP and causing only a minimal decreases in HR, while the 7-methoxychromone **25** remarkably achieved drug levels of 158 ± 13 μg/g in the brain without affecting MAP or HR (Figure 5). Further studies in DIO mice confirmed this excellent profile, affording excellent overall exposure in the plasma and brain following a single oral dose of 10 mg/kg (plasma AUC 18.7 μg·h/mL; brain AUC 4·4 μg·h/g). On the basis of its potent MCHr1 antagonist activity, in addition to its extraordinary safety against cardiovascular endpoints at high drug concentrations in the brain, the chromone-substituted aminopiperidine amide chemotype was selected as a chemical series worthy of further lead optimization. The strategic shift in lead optimization work flow (Chart 3) incorporating early assessment of cardiovascular safety by whole animal screening led to the expedient identification of the chromone-substituted aminopiperidine amides as a series worthy of further lead optimization. A full description of lead optimization activities focused on this chemotype will be disclosed in future publications.

Conclusion

Screening for cardiovascular safety early in the lead selection process using an inactin-anesthetized rat model provided an efficient means to eliminate MCHr1 antagonists that demonstrated cardiovascular liabilities. Compounds were triaged by their effects on cardiovascular endpoints and pharmacokinetic parameters. Compounds were required to achieve at least 40 μM concentration in plasma and 20 μg/g concentration in brain with less than 15% change on cardiovascular endpoints compared to vehicle responses in order to advance to further lead optimization. As a result, over 130 compounds representing multiple structurally distinct series were narrowed down to a single chemical series that achieved a favorable cardiovascular profile with high exposures in plasma and brain. This report highlights the value of positioning in vivo cardiovascular safety screening early in the lead selection process. Traditional approaches typically have reserved cardiovascular safety evaluation for advanced stage candidate selection. However, the current climate of drug discovery requires a thorough understanding of the safety profile of compounds as early and as quickly as possible. In this report, we have shown that creative application of established experimental approaches can expedite the discovery of safe compounds and facilitate optimization of resources for later stage testing.

Experimental Section

General. Unless otherwise specified, all solvents and reagents were obtained from commercial suppliers and used without further purification. All reactions were performed under nitrogen atmosphere unless specifically noted. Normal-phase flash chromatography was performed using Merck silica gel 60 (230−400 mesh) from E. M. Science or on a hybrid system employing Gilson components and Biotage prepacked columns. Following workup, reaction mixtures were dried over $MgSO_4$ or Na_2SO_4, filtered through a fritted glass funnel or a plug of cotton, and concentrated with a rotary evaporator at ca. 15 mmHg, warming when necessary. Thin-layer chromatography systems were the same as those used for column chromatography, with R_f approximately = 0.3. Analytical reversed-phase chromatography was performed using a Zorbax SP−C18 5μM 4.6 × 250 mm column with UV detection analyzed at 254 nM. Analytical method: (water with 0.1% TFA and CH_3CN gradient) 0−100% CH_3CN over 18 min at 1.5 mL/min. Analytical LC-MS was performed on a Shimadzu HPLC system with a Zorbax SB−C8, 5 μm 2.1 × 50 mm (Agilent technologies) column equipped with a PE Sciex, API 150EX single quadropole mass spectrometer, at a flow rate of 1 mL/min (0.05% NH_4OAc-buffer: CH_3CN and 0.05% HCOOH in H_2O:CH_3CN). UV analysis was performed at 220 and 254 nM. ^1H NMR spectra were recorded at 300 MHz unless specified otherwise; all values are referenced to tetramethylsilane as internal standard and are reported as shift (multiplicity, coupling constants in Hz, proton count) Mass spectral analysis is accomplished using fast atom bombardment (FAB-MS), electrospray (ESI-MS) or direct chemical ionization (DCI-MS) techniques. Elemental analyses were obtained at QTI Laboratories.

The synthesis and characterization of compounds **1**, **2**,[10] **3**, **4**,[11] and **12**[13] have been reported elsewhere.

Abbreviations. NH_4Cl, ammonium chloride; DMF, dimethyl formamide; Et_3N, triethylamine; EtOAc, ethyl acetate; EtOH, ethyl alcohol; MeOH, methyl alcohol; EDCI, *N*-(3-dimethylaminopropyl)-*N*′-ethylcarbodiimide; HOBt, 1-hydroxybenzotriazole hydrate; NMM, 4-methylmorpholine; AcOH, acetic acid; IPA, isopropyl alcohol; CH_3CN, acetonitrile; CH_2Cl_2, methylene chloride; $CHCl_3$, chloroform; PhMe, toluene; TFA, trifluoracetic acid.

General Procedures. Synthesis of Indazole Amides/Ureas. Method A. Alkylation of Nitroindazoles. The desired nitroindazole (18.4 mmol) was dissolved in dry DMF (0.300 M) and K_2CO_3 (2.95 equiv) was added. The mixture was stirred for 30 min, and then 1-(2-chloroethyl)pyrrolidine hydrochloride (1.54 equiv) was added. The reaction mixture was heated to 60 °C for 6−8 h and then cooled to room temperature. The reaction mixture was filtered through a plug of silica gel and rinsed with EtOAc:Et_3N (4:1). The filtrate was concentrated in vacuo to remove DMF, and the residue was purified by flash chromatography (60−100% EtOAc (w/5% Et_3N) in hexanes) to afford the individual N^1- and N^2-alkylated nitroindazoles.

Method B. Reduction of Nitroindazoles. The desired alkylated indazole (7.30 mmol), iron powder (10.0 equiv), and NH_4Cl (0.500 equiv) were suspended in a 4:1 solution of EtOH:H_2O (0.100 M).

The reaction mixture was heated to reflux for 3−5 h and then cooled to room temperature. The solvent was removed in vacuo, and the residue was stirred in refluxing EtOAc:Et_3N (4:1, 0.2 M) for 15 min, cooled to room temperature, and then filtered through a plug of silica gel. Rinsing with EtOAc:Et_3N (4:1) and removal of the solvents in vacuo afforded the corresponding aniline, which was used in the next reaction without further purification.

Method C. Amide Bond Formation. A 100 mL round-bottom flask was charged with the desired aniline (1.83 mmol), (4-benzyloxyphenyl)acetic acid (1.05 equiv), and DMF (0.200 M) under N_2. EDCI (1.20 equiv) and HOBt (1.20 equiv) were added, followed by NMM (2.50 equiv), and the reaction solution was stirred at room temperature for 4−6 h. Upon completion of the reaction as determined by TLC analysis, the DMF was removed in vacuo and the residue dissolved in EtOAc and washed with sat. $NaHCO_3$ (×3), brine, and water. The organic layer was then dried and filtered, and the solvents were evaporated in vacuo. The residue was then purified by column chromatography (0 to 5% MeOH in CH_2Cl_2) to afford the corresponding final product.

Method D. Urea Formation. A 250 mL round-bottom flask was charged with the appropriate aniline (4.34 mmol), 4-phenoxyphenyl isocyanate (1 equiv), and THF (60.0 mL) and the mixture stirred at 50 °C for 1 h. The mixture was cooled to room temperature, and the solvents were removed in vacuo. The resultant solid was triturated in boiling ether and collected by filtration to provide the title product.

2-(4-Methoxyphenyl)-*N*-[1-(2-pyrrolidin-1-ylethyl)-1*H*-indazol-5-yl]acetamide (11). The title compound was prepared according to Method C, substituting (4-methoxyphenyl)acetic acid for (4-benzyloxyphenyl)acetic acid (0.51 g, 76%). ^{1}H NMR (500 MHz, DMSO-d_6) δ 1.72−1.88 (m, 2 H), 1.90−2.02 (m, 2 H), 2.93−3.08 (m, 2 H), 3.43−3.56 (m, 2 H), 3.62 (s, 2 H), 3.64−3.71 (m, 2 H), 3.73 (s, 3 H), 4.66 (m, 2 H), 6.83−6.95 (m, 2 H), 7.12 (dd, J = 8.5, 1.5 Hz, 1 H), 7.22−7.32 (m, 2 H), 7.65−7.78 (m, 1 H), 8.08 (s, 1 H), 8.21−8.31 (m, 1 H), 10.38 (s, 1 H). MS (DCI/NH_3) m/z 245 $[M + H]^+$. Anal. ($C_{22}H_{26}N_4O_2$) C, H, N.

2-(4-Phenoxyphenyl)-*N*-[1-(2-pyrrolidin-1-ylethyl)-1*H*-indazol-5-yl]acetamide (13). The title compound was prepared according to Method C, substituting (4-phenoxyphenyl)acetic acid for (4-benzyloxyphenyl)acetic acid (1.8 g, 93%). ^{1}H NMR (DMSO-d_6) δ 1.59−1.63 (m, 4 H), 2.41−2.46 (m, 4 H), 2.85 (t, J = 6.8 Hz, 2 H), 3.64 (s, 2 H), 4.46 (t, J = 6.8 Hz, 2 H), 6.96−7.01 (m, 4 H), 7.12 (tt, J = 7.5, 1.0 Hz, 1 H), 7.40−7.35 (m, 4 H), 7.42 (dd, J = 9.2, 2.0 Hz, 1 H), 7.61 (d, J = 9.2 Hz, 1 H), 7.98 (d, J = 1.4 Hz, 1 H), 8.10 (d, J = 1.4 Hz, 1 H), 10.16 (s, 1 H). Anal. (C27H28N4O2) C, H, N.

***N*-(4-Phenoxyphenyl)-*N*′-[1-(2-pyrrolidin-1-ylethyl)-1*H*-indazol-5-yl]urea (15).** The title compound was prepared according to Method D (3.8 g, 79%). ^{1}H NMR (DMSO-d_6) δ 1.56−1.69 (m, 4 H), 2.41−2.48 (m, 4 H), 2.86 (t, J = 6.6 Hz, 2 H), 4.46 (t, J = 6.8 Hz, 2 H), 6.91−7.03 (m, 4 H), 7.03−7.14 (m, 1 H), 7.29−7.41 (m, 3 H), 7.44−7.52 (m, 2 H), 7.55−7.63 (m, 1 H), 7.85−8.00 (m, 2 H), 8.55−8.69 (m, 2 H). Anal. ($C_{26}H_{27}N_5O_2$) C, H, N.

***N*-(4-Phenoxyphenyl)-*N*′-[1-(2-piperidin-1-ylethyl)-1*H*-indazol-5-yl]urea (16).** 5-Nitroindazole (4.00 g, 24.5 mmol) was treated with K_2CO_3 (10.1 g, 73.6 mmol) in DMF (60.0 mL) for 30 min, and then 1-(2-chloroethyl)piperidine hydrochloric acid (6.80 g, 36.8 mmol) was added. The reaction mixture was heated to 60 °C for 6 h and then cooled to room temperature. The reaction mixture was filtered through a plug of silica gel, rinsed with EtOAc:Et_3N (4:1), and concentrated under vacuum. Purification via column chromatography (EtOAc:Et_3N 30:1) afforded 5-nitro-1-(2-piperidin-1-yl-ethyl)-1*H*-indazole (4.3 g, 64%). ^{1}H NMR (DMSO-d_6) δ 1.35 (m, 6 H), 2.36 (m, 4 H), 2.72 (t, J = 6.4 Hz, 2 H), 4.58 (t, J = 6.4 Hz, 2 H), 7.90 (d, J = 9.5 Hz, 1 H), 8.22 (dd, J = 9.5, 2.0 Hz, 1 H), 8.40 (s, 1 H), 8.82 (d, J = 2.0 Hz, 1 H). MS (DCI/NH_3) m/z 275 $[M + H]^+$.

A mixture of 5-nitro-1-(2-piperidin-1-yl-ethyl)-1*H*-indazole (4.30 g, 15.7 mmol), iron powder (8.80 g, 157 mmol), and NH_4Cl (423 mg, 7.80 mmol) was suspended in 80% EtOH (70 mL). The reaction mixture was heated to reflux for 3 h and then cooled to room temperature. After removing the solvents in vacuo, the residue was taken up and stirred in 4:1 EtOAc:Et_3N (30 mL) for 15 min and then filtered through a plug of silica gel, rinsing with 4:1 EtOAc:Et_3N. The filtrate was concentrated to afford a pale orange oil (3.4 g, 90%). ^{1}H NMR (DMSO-d_6) δ 1.35 (m, 2 H), 1.43 (m, 4 H), 2.36 (m, 4 H), 2.64 (t, J = 6.8 Hz, 2 H), 4.35 (t, J = 6.8 Hz, 2 H), 4.76 (s, 2H), 6.72 (dd, J = 2.0, 0.7 Hz, 1 H), 6.79 (dd, J = 8.8, 2.0 Hz, 1 H), 7.34 (d, J = 8.8 Hz, 1 H), 7.67 (d, J = 1.0 Hz, 1 H). MS (DCI/NH_3) m/z 245 $[M + H]^+$.

The title compound was prepared by reacting 4-phenoxyphenyl isocyanate (50 mg, 0.23 mmol) with 1-(2-piperidin-1-yl-ethyl)-1*H*-indazol-5-ylamine (58 mg, 0.23 mmol) at room temperature for 1 h. The solvent was removed in vacuo, and the residue was triturated in boiling ether. A pale white solid was obtained upon suction filtration (85 mg, 80%). ^{1}H NMR (DMSO-d_6) δ 1.34 (m, 2 H), 1.43 (m, 4 H), 2.39 (s, 4 H), 2.70 (s, 2 H), 4.46 (m, 2 H), 6.94−7.00 (m, 4 H), 7.06−7.11 (m, 1 H), 7.48 (d, J = 9.2 Hz, 3 H), 7.58 (d, J = 8.9 Hz, 1 H), 7.88 (d, J = 1.5 Hz, 1 H), 7.96 (s, 1 H), 8.61 (s, 1H), 8.66 (s, 1 H). MS (DCI/NH_3) m/z 456 $[M + H]^+$. Anal. ($C_{27}H_{29}N_5O_2$) C, H, N.

1-(2,2-Dimethoxy-ethyl)-1*H*-indazol-5-ylamine (18a). To a 250 mL round-bottom flask with a stir bar were added 3.00 g (18.4 mmol) of 5-nitroindazole, 61 mL of DMF, and 5.08 g (36.9 mmol) of K_2CO_3. To this mixture was added 3.42 g (20.2 mmol) of 2-bromo-1,1-dimethoxy-ethane, and the mixture slowly heated to 55 °C and allowed to stir for 12 h. After this time, the reaction mixture was cooled to room temperature and the contents filtered over a bed of Celite. The filtrate was then evaporated to dryness and the residue purified via column chromatography (30−80% EtOAc:hexanes) to afford 2.00 g of the N^1-alkylated nitroindazole intermediate.

To a 100 mL round-bottom flask with a stir bar were added 2.00 g (7.96 mmol) of this material, NH_4Cl (0.210 g, 3.96 mmol), and 80% EtOH (70.0 mL). To this was added 4.40 g (78.4 mmol) of iron powder, and the mixture was slowly heated to reflux. After stirring for 1 h, the reaction mixture was cooled to room temperature. The solvents were evaporated, and the residue was taken up in 10:1 EtOAc:Et_3N and filtered over a plug of silica gel, eluting with the same mixture. Evaporation of the solvents afforded 1.8 g of a pale yellow oil (38% from 5-nitroindazole). ^{1}H NMR (DMSO-d_6) δ 3.16−3.28 (m, 6 H), 4.35 (d, J = 5.4 Hz, 2 H), 4.71 (t, J = 5.6 Hz, 1 H), 4.81 (s, 2 H), 6.66−6.76 (m, 1 H), 6.80 (dd, J = 8.8, 2.0 Hz, 1 H), 7.35 (d, J = 8.8 Hz, 1 H), 7.72 (s, 1 H). MS (ESI) m/z 222 $[M + H]^+$.

***N*-(4-Phenoxyphenyl)-*N*′-[1-(2-azepan-1-yl-ethyl)-1*H*-indazol-5-yl]urea (19).** A mixture of 18a (1.00 g, 4.52 mmol), 4-phenoxyphenyl isocyanate (0.955 g, 4.52 mmol), and THF (60.0 mL) was heated to 60 °C for 1 h. The mixture was cooled to room temperature and concentrated under reduced pressure to provide a brown solid. The residue was triturated from boiling ether to provide 1.20 g of the urea intermediate. ^{1}H NMR (DMSO-d_6) δ 3.25 (s, 6 H), 4.46 (d, J = 5.4 Hz, 2 H), 4.75 (t, J = 5.4 Hz, 1 H), 6.89−7.04 (m, 4 H), 7.02−7.14 (m, 1 H), 7.26−7.42 (m, 3 H), 7.43−7.54 (m, 2 H), 7.55−7.65 (m, 1 H), 7.81−7.94 (m,1 H), 7.99 (s, 1 H), 8.52−8.78 (m, 2 H). MS (ESI) m/z 433 $[M + H]^+$.

A solution of this material (0.750 g, 1.74 mmol) in 2 N HCl:THF (1:1, 16.0 mL) was heated to 60 °C for 6 h after which time the reaction solution was cooled to room temperature and the solvents removed in vacuo. The residue was then taken up in PhMe and concentrated in vacuo (×3). A portion of this residue (0.042 g, 0.109 mmol) was taken up in 1.5 mL of 1:1 CH_2Cl_2:MeOH (1% AcOH), and hexamethyleneimine (0.013 g, 0.130 mmol) was added, followed by macroporous cyanoborohydride resin (155 mg, 2.1 mmol/g, 3 equiv). The reaction mixture was shaken at 40 °C for 3 h, cooled to room temperature, and filtered. The filtrate was concentrated under reduced pressure and purified by preparative HPLC to provide the title product (0.022 g, 42%). ^{1}H NMR (DMSO-d_6) δ 1.46 (m, 8 H), 2.60 (m, 4 H), 2.92 (t, J = 6.6 Hz, 2 H), 4.41 (t, J = 6.6 Hz, 2 H), 6.94−6.99 (m, 4 H), 7.06−7.11 (m, 1 H), 7.32−7.38 (m, 3 H), 7.48 (d, J = 9.2 Hz, 2 H), 7.59 (d, J =

9.2 Hz, 1 H), 7.87 (m, 1 H), 7.95 (d, $J = 0.9$ Hz, 1 H), 7.96 (s, 1 H), 8.59 (s, 1 H), 8.63 (s, 1 H). Anal. ($C_{28}H_{31}N_5O_2$) C, H, N.

2-(2,2-Dimethoxyethyl)-2H-indazol-5-ylamine (18b). The corresponding nitroindazole was isolated via column chromatography from the reaction described in example **18a** (1.08 g). ^{1}H NMR (400 MHz, DMSO-d_6) δ 3.31 (s, 6 H), 4.67 (d, $J = 5.5$ Hz, 2 H), 4.91 (t, $J = 5.5$ Hz, 1 H), 7.81 (m, 1 H), 7.98 (m, 1 H), 8.62 (m, 2 H); MS (DCI/NH_3) m/z 252 $[M + H]^+$.

The title product was prepared via iron reduction according to example **18a** (0.96 g, 23% from 5-nitroindazole). ^{1}H NMR (DMSO-d_6) δ 3.27 (s, 6 H), 4.38 (d, $J = 5.8$ Hz, 2 H), 4.81 (m, 3 H), 6.56 (m, 1 H), 6.75 (m, 1 H), 7.33 (m, 1 H), 7.87 (s, 1 H). MS (DCI/NH_3) m/z 222 $[M + H]^+$.

***N*-(4-Phenoxyphenyl)-*N*′-[2-(2-pyrrolidin-1-ylethyl)-2*H*-indazol-5-yl]urea (17).** The title compound was prepared according to Method D (2.3 g, 51%). ^{1}H NMR (DMSO-d_6) δ 1.66 (m, 4 H), 2.50 (m, 4 H), 2.96 (m, 2 H), 4.48 (t, $J = 5.9$ Hz, 2 H), 6.97 (m, 4 H), 7.11 (m, 2 H), 7.36 (m, 2 H), 7.50 (m, 3 H), 7.88 (m, 1 H), 8.26 (s, 1 H), 8.54 (s, 1 H), 8.64 (s, 1 H). Anal. ($C_{26}H_{27}N_5O_2$) C, H, N.

***N*-{2-[2-(3-(*S*)-Hydroxypyrrolidin-1-yl)ethyl]-2*H*-indazol-5-yl}-*N*′-(4-phenoxyphenyl)urea (20).** A mixture of **18b** (0.600 g, 2.71 mmol) and 4-phenoxyphenyl isocyanate (0.573 g, 2.71 mmol) in THF (36.0 mL) was heated to 60 °C for 1 h. The mixture was cooled to room temperature and concentrated under reduced pressure to provide a brown solid. The residue was triturated from boiling ether to provide 1.10 g of the urea intermediate. ^{1}H NMR (DMSO-d_6) δ 3.29 (s, 6 H), 4.48 (d, $J = 5.4$ Hz, 2 H), 4.74−4.92 (m, 1 H), 6.90−7.02 (m, 4 H), 7.04−7.20 (m, 2 H), 7.30−7.40 (m, 2 H), 7.44−7.59 (m, 3 H), 7.84−7.92 (m, 1 H), 8.22 (s, 1 H), 8.46−8.70 (m, 2 H). MS (ESI) m/z 433 $[M + H]^+$.

A solution of this material (0.750 g, 1.74 mmol) in 2 N HCl:THF (1:1, 16 mL) was heated to 60 °C for 6 h after which the solvents were removed in vacuo. A portion of the residue was then taken up in PhMe and concentrated in vacuo (×3). 1-[2-(2-Oxoethyl)-2*H*-indazol-5-yl]-3-(4-phenoxyphenyl)urea (50.0 mg, 0.130 mmol), (*S*)-3-pyrrolidinol (21.0 μL, 0.26. mmol), 1 M sodium cyanoborohydride in THF (260 μL, 0.260 mmol), and THF (4.00 mL) were then added, and the mixture shaken at room-temperature overnight. The solution was concentrated and purified via RP-HPLC to afford the final product (8.0 mg, 14%). ^{1}H NMR (DMSO-d_6) δ 1.45−1.57 (m, 1 H), 1.91 (ddd, $J = 13.1$, 7.5, 6.9 Hz, 1 H), 2.32 (dd, $J = 9.5$, 3.7 Hz, 1 H), 2.54−2.66 (m, 1 H), 2.73 (dd, $J = 9.5$, 6.1 Hz, 1 H), 2.94 (t, $J = 6.4$ Hz, 2 H), 3.27−3.29 (s, 1 H), 4.15 (td, $J = 7.0$, 3.6 Hz, 1 H), 4.45 (t, $J = 6.4$, 2 H), 4.66 (d, $J = 4.4$ Hz, 1 H), 6.93−7.02 (m, 4 H), 7.04−7.16 (m, 2 H), 7.32−7.40 (m, 2 H), 7.44−7.56 (m, 3 H), 7.88 (s, 1 H), 8.25 (s, 1 H), 8.53 (s, 1 H), 8.63 (s, 1 H). MS (ESI) m/z 458 $[M + H]^+$. Anal. ($C_{26}H_{27}N_5O_3$) C, H, N.

Synthesis of 4-Aminopiperidine Heterocycles. 1-(1,3-Benzodioxol-5-ylmethyl)piperidin-4-amine (22). AcOH (2.00 mL) was added to a suspension of 4-*N*-Boc-aminopiperidine (5.00 g, 25.0 mmol), piperonal (3.75 g, 25.0 mmol), sodium sulfate (7.10 g, 500 mmol), and THF (100 mL). After 20 min, sodium triacetoxyborohydride (10.6 g, 50.0 mmol) was added. After 16 h, MeOH (4.00 mL) was added and the mixture was stirred for 24 h. The solution was diluted with CH_2Cl_2 (150 mL), washed with 1 N aqueous NaOH and brine, dried ($MgSO_4$), filtered, and concentrated under reduced pressure to provide a white solid (9.00 g). This material was dissolved in CH_2Cl_2 (50.0 mL), cooled to 0 °C, and combined with TFA (25.0 mL). The mixture was stirred for 1 h and concentrated under reduced pressure and the residue combined with 2 M HCl in ether (30.0 mL) and ether (30.0 mL). The resulting white precipitate was collected by filtration and air-dried overnight to provide the title compound as the dihydrochloride salt. ^{1}H NMR (DMSO-d_6) δ 1.94 (m, 2 H), 2.06 (m, 2 H), 2.95 (m, 2 H), 3.21 (m, 2 H), 3.40 (m, 1 H), 4.14 (d, $J = 5.4$ Hz, 2 H), 6.07 (s, 2 H), 6.99 (m, 2 H), 7.24 (s, 1 H), 8.28 (s, 2 H); MS (APCI) m/z 235 $[M + H]^+$.

***N*-(1-Benzo[1,3]dioxol-5-ylmethyl-piperidin-4-yl)-5-chloro-2-(2-isopropoxyethylamino)nicotinamide (5a).** A solution of 2,5-dichloronicotinic acid (0.090 g, 0.47 mmol), EDCI (0.090 g, 0.47 mmol), and HOBt (0.060 g, 0.47 mmol) in CH_2Cl_2 (10 mL) was stirred at room temperature for 10 min. **22** (0.10 g, 0.43 mmol) was added and the solution stirred at room temperature for 12 h. The reaction was diluted with saturated $NaHCO_3$ (20 mL) and the organic layer collected, dried over $MgSO_4$, and evaporated to afford a white solid (0.17 g, 95%). ^{1}H NMR (DMSO-d_6) δ 1.55 (m, 2 H), 1.81 (m, 2 H), 2.12 (m, 2 H), 2.72 (m, 2 H), 3.42 (s, 2 H), 3.72 (m, 1 H), 6.00 (s, 2 H), 6.78 (m, 1 H), 6.82 (m, 2 H), 8.14 (s, 1 H), 8.58 (s, 1 H), 8.6 (br s, 1 H). MS (ESI) m/z 408 $[M + H]^+$.

A portion of this material (0.140 g, 0.340 mmol) was dissolved in CH_3CN (5 mL), and 2-isopropoxyethylamine (0.110 g, 1.02 mmol) was added. The reaction solution was heated to 150 °C for 30 min in a CEM Explorer microwave. The solvent was evaporated and the residue purified via column chromatography on silica gel using 5% MeOH in CH_2Cl_2 to afford the title product as a white solid. (50 mg, 31%). ^{1}H NMR, (DMSO-d_6) δ 1.08 (d, 6 H), 1.54 (m, 2 H), 1.75 (m, 2 H), 1.98 (m, 2 H), 2.79 (m, 2 H), 3.39 (s, 2 H), 3.49 (m, 4 H), 3.55 (m, 1 H), 3.69 (m, 1 H), 5.98 (s, 2 H), 6.72−7.76 (m, 1 H), 6.83−6.85 (m, 2 H), 8.01 (m, 1 H), 8.15 (m, 1 H), 8.34 (s, 1 H), 8.38 (m, 1 H). Anal. ($C_{24}H_{31}ClN_4O_4$) C, H, N.

***N*-(1-Benzo[1,3]dioxol-5-ylmethyl-piperidin-4-yl)-5-chloro-2-[(thiazol-2-ylmethyl)amino]benzamide (6).** A solution of 5-chloroisatoic anhydride (0.250 g, 1.26 mmol) and **22** (0.400 g, 1.28 mmol) were heated at 80 °C for 24 h. The reaction solution was cooled to room temperature, diluted with water (25 mL), and extracted with EtOAc (3 × 25 mL). The organic extracts were washed with water (5 × 20 mL), dried over $MgSO_4$, and evaporated to afford a clear oil that was carried forward to the next step.

This material was placed along with thiazole-2-carbaldehyde (0.170 g, 1.51 mmol) in THF (with 2% AcOH, 15 mL) and heated at reflux for 15 h. The reaction mixture was then cooled to room temperature, sodium triacetoxyborohydride (0.830 g, 3.90 mmol) was added, and the reaction mixture was stirred at room temperature for 24 h. The reaction was quenched by the addition of saturated $NaHCO_3$ (25 mL) and water (20 mL) and extracted with EtOAc (3 × 30 mL). The organic extracts were washed with water (20 mL) and dried over $MgSO_4$. The solvent was evaporated and the residue purified via reverse phase HPLC to afford a foamy white solid. This material was taken up in EtOAc and washed with saturated $NaHCO_3$ (2 × 25 mL). The organic layers were dried over $MgSO_4$ and evaporated to afford a white foam. The foamy material was crystallized from EtOAc/MeOH to afford the title compound (0.13 g, 21%) as white needles. ^{1}H NMR (500 MHz, DMSO-d_6) δ 1.50−1.60 (m, 2 H), 1.74−1.78 (m, 2 H), 1.99−2.06 (m, 2 H), 2.75−2.87 (m, 2 H), 3.68−3.81 (m, 1 H), 4.72 (d, $J = 6.1$ Hz, 2 H), 5.99 (s, 2 H), 6.66 (d, $J = 8.9$ Hz, 1 H), 6.73−6.8 (m, 1 H), 6.82−6.90 (m, 2 H), 7.26 (dd, $J = 8.9$, 2.5 Hz, 1 H), 7.61 (d, $J = 3.4$ Hz, 1 H), 7.62 (d, $J = 2.5$ Hz, 1 H), 7.74 (d, $J = 3.4$ Hz, 1 H), 8.33 (m, 1 H), 8.39 (m, 1 H). EIMS: 485.2 ($M^+ + H$). Anal. ($C_{24}H_{25}ClN_4O_3S$) C, H, N.

(1-Benzo{1,3}dioxol-5-ylmethyl-piperidin-4-yl)(5-chloro-1*H*-indazol-3-yl)amine (7). The product was prepared according to ref 13. ^{1}H NMR (DMSO-d_6) δ 1.35−1.57 (m, 2 H), 1.86−2.11 (m, 4 H), 2.70−2.87 (m, 2 H), 3.38 (s, 2 H), 3.41−3.55 (m, 1 H), 5.82 (m, 1 H), 5.98 (s, 2 H), 6.70−6.79 (m, 1 H), 6.80−6.90 (m, 2 H), 7.04−7.34 (m, 2 H), 7.64−7.97 (m, 1 H), 11.52 (s, 1 H). Anal. ($C_{20}H_{21}ClN_4O_2$) C, H, N.

(1-Benzo{1,3}dioxol-5-ylmethylpiperidin-4-yl)(6-methoxyquinolin-4-yl)amine (23). A vial was charged with $Pd(OAc)_2$ (0.010 equiv, 0.020 mmol, 5.0 mg), *rac*-BINAP (0.015 equiv, 0.003 mmol, 20 mg), and PhMe (1.0 mL) and stirred for 15 min. 1-Benzo[1,3]-dioxol-5-ylmethylpiperidin-4-ylamine (**22**, 1.10 equiv, 2.30 mmol, 541 mg) was added, and the reaction was stirred for an additional 15 min. An additional 2 mL of PhMe was added, followed by 4-bromo-6-methoxyquinoline (1.00 equiv, 2.10 mmol, 500 mg), and NaO*t*Bu (1.40 equiv, 2.90 mmol, 282 mg). The reaction was stirred at 80 °C until the 4-bromo-6-methoxyquinoline was consumed, as determined by HPLC analysis (1 h), and then cooled to room temperature. The solids were isolated by filtration (supernatant levels of product were 1.4 mg/mL), suspended in hot IPA (5 mL),

and water (5 mL) was added dropwise. The resulting suspension was cooled to room temperature and stirred for 1 h (supernatant = 3.6 mg/mL). The suspension was filtered, and the wet cake was washed with water and then dried at 50 °C, 20 mmHg. The product was obtained as an off-white solid (0.53 g, 64% yield). ^{1}H NMR (DMSO-d_6) δ 1.54−1.75 (m, 2 H), 1.90−2.03 (m, 2 H), 2.03−2.16 (m, 2 H), 2.80−2.92 (m, 2 H), 3.37−3.45 (m, 2 H), 3.46−3.55 (m, 1 H), 3.89 (s, 3 H), 5.99 (s, 2 H), 6.39−6.50 (m, 1 H), 6.50−6.59 (m, 1 H), 6.71−6.80 (m, 1 H), 6.82−6.90 (m, 2 H), 7.24 (dd, J = 9.2, 2.7 Hz, 1 H), 7.53−7.60 (m, 1 H), 7.63−7.71 (m, 1 H), 8.24 (d, J = 5.1 Hz, 1 H). Anal. ($C_{23}H_{25}N_3O_3$) C, H, N.

***N*-[1-(1,3-Benzodioxol-5-ylmethyl)piperidin-4-yl]-6,7-dichloro-4-oxo-4*H*-chromene-2-carboxamide (24).** A solution of 6,7-dichloro-4-oxo-4*H*-chromene-2-carboxylic acid (0.065 g, 0.25 mmol) and **22** (0.062 g, 0.26 mmol) in DMF (1 mL) was charged with HOBt (0.036 g, 0.26 mmol), Et_3N (38 μL, 0.28 mmol), and EDCI (0.053 g, 0.28 mmol). The resultant homogeneous solution was stirred at room temperature for 18 h, diluted with EtOAc, washed with water, 1 M K_2CO_3, and brine, dried (Na_2SO_4), and concentrated to give a beige powder. Purification by flash silica gel chromatography (0 to 5% MeOH in CH_2Cl_2) provided the title compound as a white powder (86 mg, 72%). ^{1}H NMR (DMSO-d_6) δ 1.54−1.69 (m, 2 H), 1.76−1.84 (m, 2 H), 1.95−2.07 (m, 2 H), 2.83 (d, J = 11.9 Hz, 2 H), 3.37−3.41 (m, 2 H), 3.78 (d, J = 7.8 Hz, 1 H), 5.99 (s, 2 H), 6.73−6.77 (m, 1 H), 6.83−6.89 (m, 3 H), 8.13 (s, 1 H), 8.16 (s, 1 H), 8.82 (d, J = 8.1 Hz, 1 H). Anal. ($C_{23}H_{20}Cl_2N_2O_5$) C, H, N.

***N*-[1-(1,3-Benzodioxol-5-ylmethyl)piperidin-4-yl]-7-methoxy-4-oxo-4*H*-chromene-2-carboxamide (25).** A solution of 6-methoxy-4-oxo-4*H*-chromene-2-carboxylic acid (0.055 g, 0.25 mmol) and **22** (0.062 g, 0.26 mmol) in 1 mL of DMF was charged with HOBt (0.036 g, 0.26 mmol), Et_3N (38 μL, 0.28 mmol), and EDCI (0.053 g, 0.28 mmol). The resultant homogeneous solution was stirred at room temperature for 18 h, diluted with EtOAc, washed with distilled water, 1 M K_2CO_3, and brine, dried (Na_2SO_4), and concentrated to give an off-white powder. Purification by flash chromatography (0 to 5% MeOH in CH_2Cl_2) provided the title compound as a white powder (0.088 g, 81%). ^{1}H NMR (DMSO-d_6) δ 1.63 (m, 2 H), 1.80 (m, 2 H), 2.00 (m, 2 H), 2.85 (m, 2 H), 3.39 (bs, 2 H), 3.76 (m, 1 H), 3.93 (s, 3 H), 5.98 (s, 2 H), 6.73 (m, 2 H), 6.85 (m, 2 H), 7.10 (dd, J = 9.0, 2.5 Hz, 1 H), 7.24 (d, J = 2.4 Hz, 1 H), 7.95 (d, J = 8.8 Hz, 1 H), 8.83 (d, J = 7.8 Hz, 1 H); MS (ESI, MeOH/NH_4OH) m/z 437 [M + H], 459 [M + Na], 435 [M − H]; Anal. ($C_{24}H_{24}N_2O_6 \cdot 0.5H_2O$) C, H, N.

In Vitro Compound Evaluation. MCHR1 Binding Assay Using IMR-32 Membrane Preparations. Inhibition of binding of MCHr1 by MCH was determined using membranes prepared from IMR-32 cells transfected with the promiscuous G-protein, $G_{\alpha 16}$ (I3.4.2 cells[23]). In 96-well plates, I3.4.2 membranes (6 μg/well) were incubated in the presence of test compound in binding buffer (25 mM HEPES pH 7.4, 1 mM $CaCl_2$, 5 mM $MgCl_2$, and 0.5% (w/v) BSA) and 0.05 nM [^{125}I]MCH (PerkinElmer; 2200 Ci/mmol) per well for 60 min at room temperature. Nonspecific binding controls consisted of I3.4.2 membranes, 0.05 nM [^{125}I]MCH, and 300 nM human MCH. Total binding controls of I3.4.2 membranes and 0.05 nM [^{125}I]MCH were also included on each plate. The plates were centrifuged for 5 min at 1380g in a Beckman GS-6R desktop centrifuge. The reaction buffer was carefully aspirated from each well without disturbing the pellet. Wash buffer (25 mM HEPES pH 7.4, 1 mM $CaCl_2$, 5 mM $MgCl_2$, and 0.5 M NaCl) was added to each well and then transferred to a 0.5% polyethyleneimine-treated GF/B Filtration Plate (Packard) using a plate Filtermate Harvester (Packard). The filter plate was washed three times with wash buffer, Microscint-20 (Packard) was added to each well, and the plate was read using a TopCount microplate scintillation counter (Packard).

Assay for Release of Intracellular Ca^{2+}. Activation of MCHr1 by MCH induces the release of Ca^{2+} from intracellular stores. This release of intracellular Ca^{2+} was measured using a fluorometric imaging plate reader (FLIPR, Molecular Devices) in conjunction with a Ca^{2+}-sensitive dye reagent (Calcium Assay Reagent, Molecular Devices). Release of Ca^{2+} from intracellular stores causes an increase in fluorescence of the dye proportional to the Ca^{2+} concentration. Briefly, the assays were performed as follows. I3.4.2 cells[23] were plated at 100 000 cells/well in poly-D-lysine-coated 96-well plates. After 2 days, cells were loaded with Calcium Assay Reagent for 1 h at room temperature. Test compounds were prepared at 60 μM in 6% DMSO. The cell plate was placed in the FLIPR instrument, and 50 μL/well of test compound was delivered. The Ca^{2+} signal was followed for 3 min to assay for potential receptor agonism by the test compounds. Then, 50 μL/well of 6 μM human MCH (in D-PBS containing 0.1% BSA) was added, and the ligand-induced Ca^{2+} signal was followed for an additional 3 min. Antagonist activity, as determined by the ability of test compounds to inhibit 50% of MCH-induced Ca^{2+} flux, was reported. The percent inhibition was calculated using the formula below:

$$\% \text{ inhibition} = [1 - ((\text{fTC} - \text{fB})/(\text{fMCH} - \text{fB}))] \times 100$$

where fTC = MCH-induced fluorescence in the presence of test compound, fMCH = MCH-induced fluorescence in the absence of test compound, and fB = baseline fluorescence.

In Vivo Compound Evaluation. Pharmacokinetic Analysis of Plasma and Brain Exposure in DIO Mice. Male C57Bl/6J mice are placed on a 60% kcal lard diet for 3−4 months, during which time they become obese (45 g vs 30 g for lean controls on normal chow). Compounds are dosed in DIO-mice orally at 10 mg/kg in a vehicle containing 1% Tween-80 and water. Plasma samples are drawn, whole brains are harvested at 0.5, 1, 2, 4, 6, 8, 12, and 24 h after the dose, and drug concentrations are determined by mass spectroscopy analysis in comparison with a standard curve. The three mice with highest concentrations were averaged to provide the peak plasma or brain concentration (C_{max}) ± SEM; the time for these three samples was averaged to provide the time to peak plasma or brain concentration (T_{max}) ± SEM. The mean plasma concentration data were submitted to multiexponential curve fitting using WinNonlin. The area under the mean plasma concentration−time curve from 0 to t h (time of the last measurable plasma concentration) after dosing (AUC_{0-t}) was calculated using the linear trapezoidal rule for the plasma concentration−time profile. The residual area was extrapolated to infinity, determined as the final measured mean plasma concentration (C_t) divided by the terminal elimination rate constant (β), and added to AUC_{0-t} to produce the total area under the curve ($AUC_{0-\infty}$).

Compound Evaluation in Inactin-Anesthetized Rat Cardiovascular Assay. Male Sprague−Dawley rats 325−375 g were anesthetized with the long acting barbiturate, Inactin (100 mg/kg, ip). Catheters (PE-50) were placed in the femoral artery for measurement of mean arterial pressure (MAP) and heart rate (HR). Hemodynamic data was monitored continuously and acquired at 250 Hz at a logging rate of every 5 s, which was averaged every minute using a Ponemah software platform (Gould Instrument Systems, Valley View, OH). Post-hoc, data was further reduced to 5-min averages for each rat using the Microsoft Excel spreadsheet application. Additional catheters were placed in the femoral vein for compound administration (1−2 mL/kg) and saline infusion (10 uL/min) to maintain hydration. A large blood sample was taken after the highest dose or when MAP decreased below 70 mmHg. This minimum pressure level was implemented to ensure a functional cardiovascular system for the collection of the end-of-study (EOS) blood sample used for drug plasma level determinations. A compromised vasculature can cause venous pooling and yield unrepresentative plasma results. Escalating doses were given in half log increments, such that the complete dose was administered by the end of each 30-min infusion period. The highest doses infused were either 100 or 300 mg/kg, representing the limits of solubility achieving the highest possible plasma concentrations. All compounds were dosed using poly(ethylene glycol) 400 (PEG-400) as the vehicle. The PEG-400 vehicle produces cardiovascular effects (increasing MAP and decreasing HR), but these effects are minimally variable and highly reproducible. All cardiovascular results are expressed as mean ± SEM (n = 3 rats per compound)

graphed at 5-min timepoints relative to drug administration as described above. This level of quantitation was used to define screening of MCHr1 antagonists for cardiovascular effects.

Compound Evaluation in the Pentobarbital-Anesthetized Dog Cardiovascular Assay. Male beagle dogs (n = 3/group) were anesthetized with pentobarbital (35.0 mg/kg, iv) and immediately placed on a constant iv infusion (6.0 mg/kg/h, 0.21 mL/min) to maintain a surgical plane of anesthesia as previously described.[14] Animals were intubated with a cuffed endotracheal tube and ventilated with room air by means of a mechanical respiration pump (Harvard Apparatus, Model 613). Expiratory CO_2 was monitored with an end-tidal CO_2 monitor (Criticare Systems; Model POET TE) and maintained at 4−5%. Briefly, polyethylene catheters were inserted into the right femoral vein and artery for infusion of test agents and collection of blood samples, respectively. A Swan-Ganz catheter (5.5 F) was advanced into the pulmonary artery via the right jugular vein for measurement of cardiac output via thermodilution utilizing a cardiac output computer (Abbott Laboratories, Oximetrix 3). Central venous pressure and pulmonary arterial pressure were measured through the distal port of the catheter. A dual tip micromanometer catheter (Millar, Model SPC-770, 7F) was advanced into the left ventricle of the heart via the right carotid artery for measurement of left ventricular and aortic blood pressure. The primary hemodynamic variables were recorded using a commercial software and a signal processing workstation (Ponemah, Gould Instrument Systems, Inc). Animals were randomly divided into one of five treatment or vehicle (PEG-400) groups. Following the completion of the surgical protocol, animals were allowed to stabilize for 1 h and baseline data were collected at 5-min intervals.

Compound **4** was administered as a series of three escalating doses (0.33, 1.00, and 3.33 mg/kg/min) and was dissolved in a vehicle containing PEG-400 with 1 equiv of HCl. Following termination of the high dose infusion, the animals were observed for 1 h.

Acknowledgment. The authors thank Christopher Ogiela, Dennis Fry, and Doug Falls for preparing the IMR-32 cells and aiding with the execution of the binding and functional assays, Paul Richardson and J.J. Jiang for MCH production, and Brian Droz and Victoria Knourek-Segel for help with compound dosing.

Supporting Information Available: Detailed experimental procedures for synthesis of the compounds described in the paper; characterization data for the compounds and procedures for both in vitro and in vivo assays. This material is available free of charge via the Internet at http://pubs.acs.org.

References

(1) Saito, Y.; Nothacker, H.-P.; Civelli, O. Melanin-concentrating hormone receptor: An orphan receptor fits the key. *Trends Endocrinol. Metab.* **2000**, *11*, 299−303.

(2) Schwartz, M. W.; Woods, S. C.; Porte, D., Jr.; Selley, R. J.; Baskin, D. G. Central nervous system control of food intake. *Nature* **2000**, *404*, 661−671.

(3) Della-Zuana, O.; Presse, F.; Ortola, C.; Duhault, J.; Nahon, J. L.; Levens. N. Acute and chronic administration of melanin-concentrating hormone enhances food intake and body weight in Wistar and Sprague−Dawley rats. *Int. J. Obesity* **2002**, *26*, 1289−1295.

(4) Gomori, A.; Ishihara, A.; Ito, M.; Mashiko, S.; Matsushita, H.; Yumoto, M.; Ito, M.; Tanaka, T.; Tokita, S.; Moriya, M.; Iwaasa, H.; Kanatani, A. Chronic intracerebroventricular infusion of MCH causes obesity in mice. *Am. J. Physiol. Endocrinol. Metab.* **2003**, *284*, E583−E588.

(5) Ludwig, D. S.; Tritos, N. A.; Mastaitis, J. W.; Kulkarni, R.; Kokkotou, E.; Elmquist, J.; Lowell, B.; Flier, J. S.; Maratos-Flier, E. Melanin-concentrating hormone overexpression in transgenic mice leads to obesity and insulin resistance. *J. Clin. Invest.* **2001**, *107*, 379−386.

(6) Shimada, M.; Tritos, N. A.; Lowell, B. B.; Flier, J. S.; Maratos-Flier, E. Mice lacking melanin-concentrating hormone are hypophagic and lean. *Nature* **1998**, *396*, 670−674.

(7) Chen, Y.; Hu, C.; Hsu, C.-K.; Zhang, Q.; Bi, C.; Asnicar, M.; Hsiung, H. M.; Fox, N.; Slieker, L. J.; Yang, D. D.; Heiman, M. L.; Sh, Y. Targeted disruption of the melanin-concentrating hormone receptor-1 results in hyperphagia and resistance to diet-induced obesity. *Endocrinol*. **2002**, *143*, 2469−2477.

(8) Marsh, D. J.; Weingarth, D. T.; Novi, D. E.; Chen, H. Y.; Trumbauer, M. E.; Chen, A. S.; Guan, X.-M.; Jiang, M. M.; Feng, Y.; Camacho, R. E.; Shen, Z.; Frazier, E. G.; Yu, H.; Metzger, J. M.; Kuca, S. J.; Shearman, L. P.; Gopal-Truter, S.; MacNeil, D. J.; Strack, A. M.; MacIntyre, D. E.; Van der Ploeg, L. H. T.; Qian, S. Melanin-concentrating hormone 1 receptor-deficient mice are lean, hyperactive, and hyperphagic and have altered metabolism. *Proc. Natl. Acad. Sci. U.S.A.* **2002**, *99*, 3240−3245.

(9) (a) Borowsky, B.; Durkin, M. M.; Ogozalek, K.; Marzabadi, M. R.; DeLeon, J.; Lagu, B.; Heurich, R.; Lichtblau, H.; Shaposhnik, Z.; Daniewska, I.; Blackburn, T. P.; Branchek, T. A.; Gerald, C.; Vaysse, P. J.; Forray, C. Antidepressant, anxiolytic and anorectic effects of a melanin-concentrating hormone-1 receptor antagonist. *Nature Med.* **2002**, *8*, 779−781. (b) An orally active small molecule MCHr1 antagonist in an acute feeding model was reported in the following: Takekawa, S.; Asami, A.; Ishihara, Y.; Terauchi, J.; Kato, K.; Shimomura, Y.; Mori, M.; Murakoshi, H.; Kato, K.; Suzuki, N.; Nishimura, O.; Fujino, M. T-226296: A novel, orally active and selective melanin-concentrating hormone receptor antagonist. *Eur. J. Pharmacol*. **2002**, *438*, 129−135.

(10) Kym, P. R.; Iyengar, R.; Souers, A. J.; Lynch, J. K.; Judd, A. S.; Gao, J.; Freeman, J.; Mulhern, M.; Zhao, G.; Vasudevan, A.; Wodka, D.; Blackburn, Ch.; Brown, J.; Che, J. L.; Cullis, C.; Lai, Su J.; LaMarche, M.; Marsilje, T.; Roses, J.; Sells, T.; Geddes, B.; Govek, E.; Patane, M.; Fry, D.; Dayton, B. D.; Brodjian, S.; Falls, D.; Brune, M.; Bush, E.; Shapiro, R.; Knourek-Segel, V.; Fey, T.; McDowell, C.; Reinhart, G. A.; Preusser, L. C.; Marsh, K.; Hernandez, L.; Sham, H. L.; Collins, C. A. Discovery and Characterization of Amino-piperidinecoumarin Melanin Concentrating Hormone Receptor 1 Antagonists. *J. Med. Chem.* **2005**, *48*, 5888−5891.

(11) Souers, A. J.; Gao, J.; Brune, M.; Bush, E.; Wodka, D.; Vasudevan, A.; Judd, A. S.; Mulhern, M.; Brodjian, S.; Dayton, B.; Shapiro, R.; Hernandez, L.; Collins, C. A.; Kym, P. R. Identification of 2-(4-benzyloxyphenyl)-*N*-[1-(2-pyrrolidin-1-yl-ethyl)-1*H*-indazol-6-yl]-acetamide, an orally efficacious melanin-concentrating hormone receptor 1 antagonist for the treatment of obesity. *J. Med. Chem.* **2005**, *48*, 1318−1321.

(12) Vasudevan, A.; LaMarche, M. J.; Blackburn, C.; Che, J. L.; Luchaco-Cullis, C. A.; Lai, S.; Marsilje, T. H.; Patane, M. A.; Souers, A. J.; Wodka, D.; Geddes, B.; Chen, S.; Brodjian, S.; Falls, D. H.; Dayton, B. D.; Bush, E.; Brune, M.; Shapiro, R. D.; Marsh, K. C.; Hernandez, L. E.; Sham, H. L.; Collins, C. A.; Kym, P. R.. Identification of ortho-amino benzamides and nicotinamides as MCHr1 antagonists. *Bioorg. Med. Chem. Lett.* **2005**, *15*, 4174−4179.

(13) Vasudevan, A.; Souers, A. J.; Freeman, J. C.; Verzal, M. K.; Gao, J.; Mulhern, M. M.; Wodka, D.; Lynch, J. K.; Engstrom, K. M.; Wagaw, S. H.; Brodjian, S.; Dayton, B.; Falls, D. H.; Bush, E.; Brune, M.; Shapiro, R. D.; Marsh, K. C.; Hernandez, L. E.; Collins, C. A.; Kym, P. R. Aminopiperidine indazoles as orally efficacious melanin concentrating hormone receptor-1 antagonists. *Bioorg. Med. Chem. Lett.* **2005**, *15*, 5293−5297.

(14) Fryer R. M.; Preusser L. C.; Calzadilla S. C.; Hu Y.; Xu H.; Marsh K. C.; Cox B. F.; Lin C. T.; Gopalakrishnan M.; Reinhart G. A. (−)-(9S)-9-(3-Bromo-4-fluorophenyl)-2,3,5,6,7,9-hexahydrothieno-[3,2-b]quinolin-8(4H)-one 1,1-dioxide (A-278637), a novel ATP-sensitive potassium channel opener: Hemodynamic comparison to ZD-6169, WAY-133537 and nifedipine in the anesthetized canine. *J. Cardiovasc. Pharmacol.* **2004**, *44*, 137−147.

(15) Raheem, I. T.; Goodman, S. N.; Jacobsen, E. N. Catalytic asymmetric total syntheses of quinine and quinidine. *J. Am. Chem. Soc.* **2004**, *126*, 706−707.

(16) Compounds were tested for % inhibition @ 10 μM in a standard panel of 78 receptors and ion channels offered from CEREP (www.cerep.com).

(17) Screening of 130 MCHr1 antagonists for hERG blockade using cell-based dofetilide binding assays showed no correlation between hERG blockade and hemodynamic effects in vivo.

(18) Polakowski, J. S.; Segreti, J. A.; Cox, B. F.; Hsieh, G. C.; Kolasa, T.; Moreland, R. B.; Brioni, J. D. Effects of selective dopamine receptor subtype agonists on cardiac contractility and regional haemodynamics in rats. *Clin. Exp. Pham. Phys*. **2004**, *31*, 837−841.

(19) Reinhart G. A.; Fryer R. M.; Osinski, M. A.; Polakowski, J. S.; Cox, B. F. Gintant, G. A. Predictive, non-GLP models of secondary pharmacodynamics: putting the best compounds forward. *Curr. Opin. Chem. Biol*. **2005**, *9*, 1−8.

(20) For studies in anesthetized dogs, the minimum pressure limit tolerated was 50% reduction in the MAP relative to vehicle treated animals. For studies in inactin-anesthetized rats, the minimum pressure limit

tolerated was 70 mmHg. This minimum pressure level was implemented to ensure a functional cardiovascular system for the collection of the end-of-study blood sample used for drug plasma level determinations.

(21) Souers, A. J.; Gao, J.; Wodka, D.; Judd, A. S.; Mulhern, M. M.; Napier, J. J.; Brune, M. E.; Bush, E. N.; Brodjian, S. J.; Dayton, B. D.; Shapiro, R.; Hernandez, L. E.; Marsh, K. C.; Sham, H. L.; Collins, C. A.; Kym, P. R. Synthesis and evaluation of urea-based indazoles as melanin-concentrating hormone receptor 1 antagonists for the treatment of obesity. *Bioorg. Med. Chem. Lett.* **2005**, *15*, 2752−2757.

(22) Ma, V. V.; Balan, C.; Tempest, P. A.; Hulme, C.; Bannon, T. Abstract of Papers, 224th National Meeting of the American Chemical Society, Boston, MA.; American Chemical Society: Washington, DC, 2002; Abstract MEDI-343.

(23) Fry, D.; Dayton, B.; Brodjian, S.; Ogiela, C.; Sidorowicz, H.; Frost, L. J.; McNally, T.; Reilly, R. M.; Collins, C. A. Characterization of a neuronal cell line expressing native human melanin-concentrating hormone receptor 1 (MCHr1). *Int. J. Biochem. Cell Biol.* **2006**, in press.

JM0512286